APPLICATION OF DATA MINING TOOLS TO EXTRACT KNOWLEDGE FOR DRY REFORMING OF METHANE FROM PUBLISHED PAPERS IN LITERATURE

by
Ayşe Neslihan Şener
B.S., Chemical Engineering, Yıldız Technical University, 2012

Submitted to the Institute for Graduate Studies in
Science and Engineering in partial fulfillment of
the requirements for the degree of
Master of Science

Graduate Program in Chemical Engineering
Boğaziçi University
2015

ACKNOWLEDGEMENTS

First and foremost, I would like to express my sincerest gratitude to my supervisor, Prof. Ramazan Yıldırım, who has continuously supported me throughout my thesis with his invaluable guidance and experience and unlimited patience and tolerance. This thesis would not have been possible without his inspiration and effort.

I would like to express my very sincere gratitude to Assist. Prof. Mehmet Erdem Günay for his sincere, technical and informative support during the progression of this study. I would like to offer my very special thanks to Assist. Prof. Mustafa Gökçe Baydoğan for his kind interests during the course of Statistical Learning for Data Mining and also he gave me valuable suggestions in my thesis defense. Special thanks to Prof. Erhan Aksoylu for his valuable comments to my thesis.

Very special thanks to Manouchehr Nadjafi for his friendship, endless support and motivation, even if he is in Iran. Special thanks to Mohammad Beygi for his help during the presentation day. I would like to thank to all of my friends for their friendship, support and motivation.

Endless thanks to my family for their motivation, encouragement and every kind of support all through my life.

I would like to acknowledge the financial support of TÜBİTAK during my thesis status through 2211 National Support Programme for Master Students.

ABSTRACT

APPLICATION OF DATA MINING TOOLS TO EXTRACT KNOWLEDGE FOR DRY REFORMING OF METHANE FROM PUBLISHED PAPERS IN LITERATURE

The aim of this thesis is to extract knowledge for dry reforming of methane reaction using data mining techniques that are decision trees and artificial neural networks. Firstly, the experimental data were collected from 101 papers published between 2005 and 2014. The data set consisted of 5521 data points with 63 variables. The conversion of methane as a function of catalyst preparation and operational variables was modeled in MATLAB. CH_4 conversion values were classified as 0-50, 50-75 and 75-100 for the decision tree analyses of total data, and Ni, Co, Pt and wet impregnation bases subsets. Training and testing errors of these trees were 21.1%-21.5%, 16.7%-19.0%, 10.2%-10.9%, 9.3%-12.6%, and 13.6%-15.1%, respectively. The neural networks were also used for modeling data; tansig was used as activation function and trainlm and trainbr were used as training algorithms for training and testing, respectively. The optimal neural network topology was found as 63-20-1 (20 neuron in hidden layer) using the prediction ability of testing result. R^2 and corresponding RMSE values for training and testing were found to be 0.97-4.23 and 0.89-8.66, respectively. The relative significances of input variables were also determined using the optimal neural network topology. It was found that reaction temperature was the most significant variable, and operational variables had higher group significance than the catalyst design variables within the range of data set. Finally, the optimal neural network topology was used to predict the results of experiments and papers. 590 out of 753 experiments (78.4%) were predicted with RMSE values lower than 15. The results of 46 out of 101 papers (45.5%) were predicted with R^2 values higher than 0.5 and the RMSE values of 65 out of 101 papers (64.4%) had lower than 15.

ÖZET

VERİ MADENCİLİĞİ TEKNİKLERİNİN METANIN KURU REFORMLANMASI İLE İLGİLİ LİTERATÜRDE YAYINLANMIŞ MAKALELERDEN BİLGİ ÇIKARIMINDA KULLANILMASI

Bu tezin amacı veri madenciliği tekniklerinden karar ağaçları ve yapay sinir ağları kullanılarak metanın kuru reformlanması reaksiyonu için bilgi çıkarmaktır. İlk olarak 2005 ve 2014 yılları arasında yayınlanmış 101 makaleden deneysel veriler toplanmıştır. Veri seti 5521 veri noktasından ve 63 değişkenden oluşmaktadır. Metanın dönüşümü, katalizör hazırlama ve operasyon değişkenlerinin fonksiyonu olarak MATLAB' de modellenmiştir. Toplam veri seti ile birlikte Ni, Co, Pt ve ıslak emdirme temelli alt veri setlerinin karar ağaçları analizi yapılırken metanın dönüşümü değerleri 0-50, 50-75, 75-100 olarak sınıflandırılmıştır. Bu ağaçların eğitim ve test hataları sırasıyla %21.1-%21.5, %16.7-%19.0, %10.2-%10.9, %9.3-%12.6 ve %13.6-%15.1 olarak bulunmuştur. Ayrıca, veri setleri sinir ağları kullanılarak da modellenmiştir. Bunun için aktivasyon fonksiyonu olarak tansig kullanılırken eğitim için trainlm, test için ise trainbr eğitici algoritmaları tercih edilmiştir. En uygun sinir ağ yapısı test analizi sonucu (tahmin edebilme gücü) kullanılarak 63-20-1 (gizli katmanda 20 nöron) olarak bulunmuştur. R^2 ve bununla ilişkili RMSE değerleri sırasıyla eğitim için 0.97-4.23 ve test için 0.89-8.66 bulunmuştur. Ayrıca giren değişkelerin göreceli önem analizleri en uygun sinir ağ yapısı kullanılarak belirlenmiştir. Reaksiyon sıcaklığı en önemli değişken olarak bulunmuştur, ayrıca operasyon değişkenlerinin katalizör tasarlama değişkenlerinden daha yüksek grup önemine sahip oldukları belirlenmiştir. Son olarak en uygun sinir ağı yapısı deneylerin ve makalelerin sonuçlarını tahmin edebilmek için kullanılmıştır. 753 deneyden 590 ının (%78.4) RMSE değerleri 15 den küçük olarak tahmin edilmiştir. 101 makaleden 46 sının (%45.5) sonucu R^2 değerleri 0.5 den büyük olarak ve 101 makaleden 65 inin (%64.4) RMSE değerleri 15 den küçük olarak tahmin edilmiştir.

TABLE OF CONTENTS

LIST OF FIGURES

LIST OF TABLES

LIST OF SYMBOLS

R^2	Coefficient of determination
α	Momentum term
η	Learning rate
δ	Error

LIST OF ACRONYMS/ABBREVIATIONS

Calh	Calcination time
CalT	Calcination temperature
CART	Classification and regression tree
CI	Co-impregnation
CP	Co-precipitation
DRM	Dry reforming of methane
GHSV	Gas hourly space velocity
IWI	Incipient to wetness impregnation
MA	Mesoporous alumina
MSE	Mean square error
Redh	Reduction time
RedT	Reduction temperature
RMSE	Root mean square error
SG	Sol-gel
SI	Sequential impregnation
SSE	Sum of square errors
T	Reaction temperature
TOS	Time on stream
WI	Wet impregnation
W/F	Catalyst weight/feed flow rate
X	Conversion

1. INTRODUCTION

The rapid development of industry has increased the need of energy. The major sources of energy are fossil fuels that are oil, coals and natural gas. Continuously increasing consumption of fossil fuels leads to environmental problems such as global warming. With the depletion of oil supply of the world, some techniques have been investigated in order to convert natural gas, consisting primarily of methane (CH_4), into higher value products [1].

Conversion of CH_4 to synthesis gas (syngas), a mixture of carbon monoxide (CO) and hydrogen (H_2), can be carried out three different ways that are steam reforming, partial oxidation and dry (CO_2) reforming. Mixed reforming of methane can be preferred to control H_2/CO ratio in product stream changing the ratio of H_2O, CO_2 and O_2 in the feed stream [1]. When we compare these reforming processes, dry reforming of methane (DRM) has received more interests in the past decade because it converts two greenhouse gases into synthesis gas with a lower H_2/CO ratio that is desirable for the synthesis of long chain hydrocarbons and oxygenated chemicals through Fischer-Tropsch process [2].

Environmentally advantageous DRM reaction occurs with some side reactions. Coke formation during DRM mainly occurs due to unwanted side reactions, including methane decomposition favored at higher temperatures or carbon monoxide decomposition that is known as Boudouard reaction favored at lower temperatures. Carbon deposition is the most important challenge for DRM in order to achieve higher activity and better stability [3]. Another side reaction is reverse water gas shift reaction (RWGS). Water production and coke formation lead to undesirable H_2/CO ratios. DRM has a tendency toward sintering of metallic phase and support due to the highly endothermic nature of it [4].

The most common catalyst for DRM is supported nickel. However, it has a tendency to form coke on catalyst surface due to higher reforming temperature. This can result in deactivation of catalyst and/or plugging of tubes inside reactor. Although noble metals such as ruthenium and rhodium are more active and resistant to carbon deposition, nickel based catalysts have been investigated because of their lower cost and better availability

[5]. The most widely used support for DRM is γ-Al_2O_3 because of its higher thermal stability and specific surface area [6].

There is a huge amount of experimental research about dry reforming of methane in the literature. The most important variables affecting the results of this reaction are reaction temperature, base metals, support types, feed compositions, W/F ratio (catalyst weight/feed flow rate), reduction and calcination conditions, preparation methods and time on stream. Some data mining tools can be used in order to extract knowledge from the data set constructed from research publications. The results obtained from it can be used in experimental works to improve catalysts for DRM.

Data mining is the process of discovering useful information from the data. Some of the commonly used data mining tasks are description, prediction, classification, clustering, and association [7]. One of the most attractive classification methods is decision tree because of its simplicity and interpretability. Decision tree consists of decision nodes that are connected by branches and extends downward from the root node to the leaf nodes [8]. Artificial neural networks are used commonly because of their success in modeling even for very complex functions. The ability to deal with nonlinear relations among variables is a major benefit of neural networks. However, it has a lot of parameters to adjust [9].

This thesis is composed of five chapters. Detailed information about dry reforming of methane reaction and data mining techniques such as decision trees, classification and neural network algorithm are explained in Literature Survey (Chapter 2). All the details related to collection of data, construction of data set and computational details used in this thesis are given in Experimental Data and Computational Details (Chapter 3). Decision tree and artificial neural network results are presented and discussed in Results and Discussion (Chapter 4). Finally, the conclusions drawn from this study and recommendations for future studies are given in Conclusions and Recommendations (Chapter 5).

2. LITERATURE SURVEY

2.1. Dry Reforming of Methane

Dry reforming of methane reaction [Eq. (2.1)] simultaneously utilizes two greenhouse gases (CH_4 and CO_2) to produce industrially valuable syngas with the H_2/CO ratio close to unity that is suitable for the synthesis of higher value liquid [2]. DRM is a highly endothermic reaction that requires the temperature higher than 800°C in order to achieve higher activity and selectivity. DRM is followed by reverse water-gas shift reaction [Eq. (2.2)] that causes a decrease in H_2/CO ratio [5]. Other side reactions can occur because of the operating conditions such as reaction temperature and reactant partial pressure. These reactions lead to catalyst deactivation by coke deposition and/or sintering of metals. The formation of coke during DRM mainly comes from CH_4 decomposition [Eq. (2.3)] to form solid carbon on the catalyst surface and produce H_2 and carbon monoxide (CO) disproportionation [Eq. (2.4)] to form surface carbon and CO_2 [1]. While the former is an endothermic reaction favored at higher temperature and lower pressure, the latter is an exothermic reaction favored at lower temperature and higher pressure [3].

Dry reforming of methane (DRM) reaction:

$$CH_4 + CO_2 \leftrightarrow 2CO + 2H_2 \qquad \Delta H_{298K} = +247 \text{ kJmol}^{-1} \tag{2.1}$$

Reverse water-gas shift reaction (RWGS):

$$CO_2 + H_2 \leftrightarrow CO + H_2O \qquad \Delta H_{298K} = +41.2 \text{ kJmol}^{-1} \tag{2.2}$$

Methane decomposition reaction:

$$CH_4 \leftrightarrow C(s) + 2H_2 \qquad \Delta H_{298K} = +75 \text{ kJmol}^{-1} \tag{2.3}$$

CO disproportionation (Boudouard) reaction:

$$2CO \leftrightarrow C(s) + CO_2 \qquad \Delta H_{298K} = -171 \text{ kJmol}^{-1} \tag{2.4}$$

2.2. Factors Effecting Dry Reforming of Methane

Numerous studies have been reported in the literature in order to develop stable catalyst and improve operating conditions for DRM. Type and loading of the metals used, addition of promoter or other metals, preparation technique, pretreatment (calcination and reduction) conditions and choice of support are the most important factors affecting the activity, selectivity and stability of catalyst. Operating conditions such as reaction temperature and pressure, reactant composition, gas hourly space velocity and time on stream are also important because they can affect catalytic performance.

2.2.1. Effect of Metal Types and Loading

The widely used metals for DRM are Ni, Co, Pt, Pd, Ru, Rh and Ir. Many studies related to this reaction have been conducted over Ni based catalysts because of its lower cost and wide availability. However, Ni based catalysts have some problems such as catalyst deactivation due to carbon formation, sintering and metal oxidation and lower activity and selectivity [4]. Noble metal such as Ru, Rh and Pt supported catalysts are highly active and stable for DRM with resistance to coke formation than other transition metals but they are more expensive than non-noble metals and they are not feasible on an industrial scale. When all of these situations mentioned above are taken into consideration, adding noble metals into nickel based catalysts can improve the activity and stability of catalysts [1]. Apart from determining active metal type(s), metal loading is also important to prevent deactivation by formation of inactive sites on catalysts. There are published papers that were analyzed the effect of metal loading with different percentages of metal for DRM in order to determine the best active metal(s) with the best amount in terms of activity and stability.

According to Xu *et al.*, different weight percentages of nickel catalysts (3, 5, 7, 10, 15 wt. %) supported on mesoporous alumina (MA) affected the catalytic activity in DRM. When Ni amount increased from 3wt.% to 15wt.%, the conversion of CH_4 and CO_2 and the ratio of H_2/CO increased until the Ni content reached to 5wt.% at various temperatures ranged from 600 °C to 800°C at a 50 °C increment. Increasing the amount of Ni between 5-15wt. percent resulted in slight improvement in the activity because 5%Ni/MA catalyst may already provide enough active sites for reactants to achieve desired conversion levels. Large specific surface areas, big pore volumes and uniform pore structures of this catalyst provide better catalytic activity [10].

Influence of alkaline earth metal oxides (MgO, CaO and BaO) on the activity and stability of 5wt.%Ni catalyst supported on γ-Al_2O_3 in DRM were investigated in the study of Alipour *et al*. 5wt.%Ni/γ-Al_2O_3 catalyst promoted with 3wt.%MgO had the highest activity in the temperature range of 550-700 °C in terms of CH_4 and CO_2 conversion because MgO can improve the Ni dispersion by surface rearrangement, catalyst activity due to formation of $MgAl_2O_4$ and catalyst stability by reducing the carbon formation on the catalyst. However, the incorporation of Ca and Ba into Ni/γ-Al_2O_3 catalyst resulted in a decrease in catalytic activity and coke formation [2].

Özkara-Aydınoğlu and Aksoylu (2010) studied 2 wt.% La, Ce, Mn, Mg, K promoted 5 wt.%Co/ZrO_2 catalysts to increase the resistance of Co-based catalysts to coking and to improve the activity of the catalysts and found that the catalytic performances of bimetallic Co-X/ZrO_2 catalysts were affected by the type of metals because of their different dispersion properties. Unpromoted Co/ZrO_2 had high initial activity but activity loss was occurred because of carbon formation during 6 h time on stream. 5Co2La/ZrO_2 catalyst exhibited the highest stability with average activity and 5Co2Ce/ZrO_2 catalyst exhibited the highest activity with a limited loss of activity in 6 h time on stream experiments [11].

2.2.2. Effect of Support Type

Active metal is mostly introduced onto support materials to obtain supported metal catalyst. Support has a relatively high surface area and it has large and regularly shaped pores [12]. Type of support and interaction between active metal and support affect the catalytic activity and carbon deposition in dry reforming of methane reaction. The support of catalyst should have resistance to higher temperature. Support affect metal dispersion [5]. The most widely used supports for DRM are γ-Al_2O_3, SiO_2, La_2O_3, ZrO_2, TiO_2, CeO_2, MgO, MCM-41 and SBA-15.

García *et al*. (2009) were studied the effect of mixed oxide supports (ZrO_2-MgO) with different amounts of MgO content ranged from 0 to 5 wt.% on the catalytic performance of Ni/ZrO_2-MgO catalysts at 600 °C for DRM. The best amount of MgO in the catalyst in terms of CH_4 conversion was found as 0.4 wt.%. The methane conversion remained almost constant at 26% during 300 min on stream. The addition of MgO into Ni/ZrO_2 inhibited the deactivation of catalyst because of the strong interaction of metal with support of the catalyst [13].

The effect of Ce/Zr ratios on the catalytic activities of the 7 wt.%Ni/CeZr catalysts with different temperatures ranged from 600 to 800 °C was investigated in the study of Xu *et al*. (2012). The optimum Ce containing was found 50 mol% and 7 wt.%Ni/Ce50Zr50 catalyst exhibited the highest activity at each temperature [14].

2.2.3. Effect of Catalyst Preparation Method

Impregnation or precipitation techniques are used to introduce the active phase of a catalyst into the support structure. Therefore a suitable solution is prepared and introduced into the pores of the support prior to drying and calcination [12]. Impregnation or precipitation methods are important in designing active and stable catalysts for DRM. Catalysts preparation techniques used in this study are incipient to wetness impregnation, wet impregnation, co-impregnation, sequential impregnation, co-precipitation and sol gel.

In the case of impregnation, the method is based on an interaction between the surface of support and the species in solution. If the volume of solution is equal to or less than the volume of pores, the impregnation method is known as pore volume or incipient to wetness impregnation, and the method depends on keeping the species within the pores during drying. If the volume of solution is in excess from the required amount to fill the pores, the method is known as wet impregnation, and the method depends on specific interactions [12].

The effect of different impregnation strategies over Pt/ZrO_2 catalysts promoted with Ce for DRM reaction was investigated by Özkara-Aydınoğlu *et al.* While the interaction between Pt and Ce increasing the oxygen storage of the catalysts was stronger for co-impregnated Ce-Pt/ ZrO_2, sequentially impregnated catalysts led to lower interaction between Pt and Ce. Therefore co-impregnated catalysts had higher activity and resistance to carbon deposition than the sequentially-impregnated catalysts [15].

2.2.4. Effect of Pretreatment (Calcination and Reduction) Conditions

Calcination and reduction processes are significant for the performances of catalysts. Calcination is applied to catalysts in order to eliminate water, carbon dioxide or other volatile compounds. Catalysts can be calcined at different temperatures and times under the stream of air or oxygen. After the calcination of catalysts, reduction can be carried out in pure H_2 or a mixture of H_2/N_2, H_2/Ar or H_2/He at different temperatures and times.

Zhang *et al*. (2008) investigated the influence of calcination temperature on the catalytic performance of Ni/TiO_2-SiO_2 catalysts that were prepared by impregnation combined sol gel method for DRM reaction and found that the catalyst calcined at 700 °C had higher activity and stability than the catalysts calcined at 550 °C and 850 °C for 5 h [16].

Takanabe *et al*. (2005) investigated the influence of reduction temperature on the catalytic performance of 10 wt.%Co/TiO_2-anatase catalysts that were prepared by incipient to wetness impregnation and calcined at 400 °C for 4 h for DRM reaction. Before the reaction the catalysts were reduced in situ with a H_2 flow (25 ml/min) at different temperatures ranged from 700 °C to 950 °C for 1 h. The activities of the catalysts decreased with increasing reduction temperatures. The catalysts reduced at 700- 800 °C exhibited higher CH_4 conversion and stability during 25 h than the catalysts reduced at 850-950 °C [17].

2.2.5. Effect of Feed Compositions

The main reactants for dry reforming of methane reaction are CH_4 and CO_2. In some papers Ar, He and N_2 introduced into feed composition as diluent gas. The ratio of CO_2/CH_4 has a significant effect on catalyst activity, so different values of carbon dioxide to methane ratios have been studied in order to find out the optimum value for CO_2/CH_4 ratio. The ratio of CO_2/CH_4 that is higher than 1 is preferred mostly to increase methane conversion.

The effects of CH_4/CO_2 ratios on the 7 wt.%Ni-3 wt.%Co/La_2O_3-Al_2O_3 bimetallic catalysts at 800°C investigated in the study of Xu *et al*. (2010). CO_2 conversion and H_2/CO ratio increased from 60% to 99% and from 0.65 to 1.38, respectively but CH_4 conversion declined from 96% to 58% with increasing CH_4/CO_2 ratios from 1/3 to 3/1. When CH_4/CO_2 ratio was higher than or equal to 1 in the feed stream, carbon deposition by CH_4 decomposition was more than carbon elimination by CO_2. In order to prevent carbon deposition CO_2 concentration in feed stream could be increased [18].

Yasyerli *et al*. (2011) studied the effects of feed composition on the 1 wt.%Ru-Ni/MCM-41 catalyst at 600 °C with gas hourly space velocity of 36000 ml/hg_{cat}. A gaseous mixture of CO_2/CH_4/Ar with different volume ratios of 1/0.66/1.33, 1/0.5/1.5 and 1/1/1 was fed into the reactor, in which Ar was used as diluent gas. When the ratio of CO_2/CH_4 was less than 1, the coke formation and reactor blockage occurred. When the ratio of CO_2/CH_4 was higher than 1, the conversion of CH_4 increased slightly [19].

2.2.6. Effect of Gas Hourly Space Velocity

Gas hourly space velocity (GHSV) is defined as the feed flow rate over catalyst weight ratio. The performances of catalysts depend on the velocity of feed gas in dry reforming of methane reaction. Higher gas hourly space velocity can lead to rapid deactivation of catalysts and decrease the sintering of metals while lower GHSV can be preferred to reach equilibrium [5].

The effect of gas hourly space velocity over 5%Ni/γ-Al_2O_3, 5%Ni-3%Mg/γ-Al_2O_3, 5%Ni-3%Ca/γ-Al_2O_3 and 5%Ni-3%Ba/γ-Al_2O_3 catalysts at 650°C with constant feed ratio (CH_4/CO_2=1) were investigated in the study of Alipour *et al*. (2014). The conversion of CH_4 and CO_2 decreased with increasing GHSV ranged from 6000 to 18000 ml/hg_{cat} because of reduced contact time and amount of adsorbed reactant [2].

Özkara-Aydınoğlu and Aksoylu (2010) were analyzed the effect of GHSV on the catalytic activity and stability of bimetallic 5wt.%Co2wt.%La/ZrO_2 and 5wt.%Co2wt.%Ce/ZrO_2 catalysts at 650°C with constant feed ratio (CH_4/CO_2=1). With decreasing GHSV from 60000 to 15600 ml/hg_{cat}, the conversion of CH_4 and CO_2 increased and reached to 50% and %61 for La-promoted cobalt catalyst and 63% and %72 for Ce-promoted cobalt catalyst at the end of 6 h on stream [11].

Xu *et al*. (2010) investigated the effects of GHSV ranged from 3000 to 18000 ml/hg_{cat} with an increment of 3000 on the performances of 7 wt.%Ni-3 wt.%Co/La_2O_3-Al_2O_3 bimetallic catalysts and found that CO_2 and CH_4 conversion and H_2/CO ratio decreased slightly with increasing GHSV and CH_4 conversion reached maximum value at 6000 ml/hg_{cat} [18].

2.2.7. Effect of Reaction Temperature

The most important variable for dry reforming of methane reaction is temperature due to the endothermicity of the reaction. DRM requires higher temperatures to achieve higher conversion of CH_4 and CO_2. At higher temperatures, supported metal catalysts tend to deactivate due to sintering of metals or supports and carbon deposition. Therefore, to design a thermally stable catalyst having higher activity is the most important issue to carry out this environmentally and industrially advantageous reaction at the big scale [1].

Serrano-Lotina and Daza (2014) investigated the influence of reaction temperature using Ni-based catalyst obtained after calcination of hydrotalcite-like precursor. When the reaction temperature increased from 450 °C to 800 °C, CH_4 and CO_2 conversion and H_2/CO ratio increased from 9%, 11% and 0.4 to 94%, 95% and 0.98, respectively [20].

2.2.8. Effect of Pressure

Dry reforming of methane is mostly operated under atmospheric pressure because this reaction is volume-increasing reaction so higher pressures lead to a reverse reaction. Moreover, CH_4 decomposition and total amount of carbon deposited on the catalyst increases at high pressure. In the literature there are only a small number of papers analyzing the effect of pressure because of the reasons mentioned above [18].

Xu *et al*. (2010) investigated how the operating conditions affect the performances of 7 wt.%Ni-3 wt.%Co/La_2O_3-Al_2O_3 bimetallic catalysts at 800°C and found that CH_4 conversion decreased from 88.2% to 54.3% and CO_2 conversion increased slightly due to an increase in deposited carbon gasification and a decrease in RWGS with the increasing operating pressure from 1 atm to 5 atm [18].

2.2.9. Effect of Time on Stream

Time on stream analysis of catalysts has been conducted to determine the short and long term stability of catalysts. Stability is important to use catalysts effectively in industry.

According to Xu *et al*., the 10%Ni/MA catalyst exhibited not only higher catalytic activity but also excellent stability throughout 100 h long stability test under the specific reaction conditions: CH_4/CO_2=1, T=700 °C, GHSV=15000ml/hg_{cat}, 1 atm. The catalyst performed over 80% and 81% conversions of the CH_4 and CO_2, respectively. Catalyst deactivation was not observed during this time because of the large specific surface areas, big pore volumes and uniform pore structures of this catalyst. H_2/CO ratio remained steady at 0.8. The conversion of CO_2 was higher than the conversion of CH_4 because of the RWGS reaction [10].

According to Alipour *et al*. (2014), the 5%Ni-3%Mg/γ-Al_2O_3 catalyst at 700 °C exhibited high stability during 15 h time on stream. MgO promoted Ni/γ-Al_2O_3 catalysts reduced well in reaction condition because of a decrease in the reduction temperature of NiO particles. The catalyst performed over 75% and 78% conversions of the CH_4 and CO_2, respectively [2].

2.3. Data Mining Methods for Knowledge Extraction

Huge amount of data is continuously produced and collected in various fields of science, in commerce and even in everyday life using the advances in technology. However, to obtain useful information from huge data set is extremely difficult. Data mining is the process of discovering hidden information from databases. Data mining techniques are applied to small or big data set in order to extract knowledge, patterns and correlations. They can predict the outcome of a future observation using existing data set [7].

Flow diagram of knowledge discovery process from a database is shown in Figure 2.1. The input data can be collected from different sources and stored in technological devices even in our computer. Preprocessing methods such as feature selection, dimensionality reduction, normalization and data subsetting can be applied to raw data to make it more suitable for subsequent analysis. Preprocessing steps include cleaning data to remove noise, outliers and missing values, selecting features that highly affected target value and reducing dimensions. Postprocessing methods such as filtering patterns, visualization and pattern interpretation are applied to data mining results to eliminate trivial results and to integrate only valid results into information [7].

Figure 2.1. The process of knowledge discovery in databases [7].

Data mining includes a lot of ideas such as sampling, estimation and hypothesis testing from statistics, searching algorithms, modeling techniques and learning theories from artificial intelligence, pattern recognition and machine learning. Data mining methods can be applied in a variety of areas such as optimization, computation and information technology, signal processing and visualization doing some modifications [7].

Data mining tasks are generally divided into two categories as predictive and descriptive. The aim of the former is to predict the target value of independent variables known as attributes or features. The aim of the latter is to find patterns such as correlations, trends, clusters, trajectories and anomalies in data [7].

Prediction is used to construct a model for the target variable as a function of input variables. There are two types of prediction: classification where the output is discrete or categorical and regression where the output is a number. Both classification and regression are supervised learning problems because input and output values are known. The aim of prediction is to build a model that minimizes the error between the predicted and actual values of the target variable [7]. If a model that fits to the collected past data (training data) is found in data set and the future data is similar to the past data, we can make correct predictions for novel instances [21]. Simple linear regression, multiple linear regression, logistic regression, k-nearest neighbor methods, naïve Bayes, regression or classification trees, artificial neural networks and support vector machines are some of the algorithms that can be used for prediction.

In unsupervised learning, data set only has input data and there is no target value. The aim of the unsupervised learning methods is to find general properties and to see certain patterns in the input. The most common form of unsupervised learning is clustering. The aim of clustering is to find groups of closely related observations. Observations belonging to the same cluster should have higher intra-class similarity and observations belonging to the different clusters should have lower inter-class similarity in order to produce effective clusters. The most commonly discussed distinction among different types of clustering is whether the set of clusters is hierarchical or partitional. K-means clustering is an example for partitional algorithms and agglomerative and divisive clustering are some of the methods for generating hierarchical clustering. Clustering can be used as a preprocessing step for other algorithms [7].

2.3.1. Classification by Decision Trees

The aim of classification is to build classification models using an input data set. Each classification technique uses learning algorithm to find a model that fits the input data well and predicts the class labels of previously unknown records accurately. After a classification model is built using the training set including features and class labels of the instances, this model can be applied to test set consisting of features of instances without their class labels [7].

Decision tree is widely used technique for classification because of its simplicity and interpretability. It is a nonparametric method. Most of the decision tree algorithms use divide-and-conquer partitioning strategy [21]. Decision tree techniques are computationally inexpensive even for larger data set. When a decision tree built, classification of test set is very fast [7]. Hunt's algorithm, CART (Classification and regression tree), ID3, C4.5 and its successor C5.0, J48 are some of the decision tree algorithms.

Each decision tree consists of root node, internal nodes and leaf or terminal nodes. Attribute test conditions are applied in nodes except for terminal nodes to separate instances. When a decision tree is constructed, classifying a test instance is easy [7]. A decision tree starts from root node and test condition is applied to the instance and then depends on the results of the test, appropriate branch of the tree is followed. This process is repeated recursively until a leaf node is reached. Each branch generates another internal node or a leaf node. Each terminal node consists of one class [21].

The main problem for a decision tree is to decide how to split records. There are many measures in order to determine the best split. The ratio between wrong classifications and total records in any node is minimized. Before and after splitting, the degree of impurity of the child nodes (when a node p split into k partitions) can be used to select the best split. Impurity is a measure of how homogenous group of observations in terms of class distribution. The most widely used node impurity measures are shown in Equation 2.5, Equation 2.6 and Equation 2.7. When the impurity level of a node decreases, the Gini index decreases [7].

$$Entropy(t) = -\sum_{i=0}^{c-1} p(i|t)\log_2 p(i|t) \tag{2.5}$$

$$Gini(t) = 1 - \sum_{i=0}^{c-1} [p(i|t)]^2 \tag{2.6}$$

$$Classification\ error(t) = 1 - \max_i [p(i|t)] \tag{2.7}$$

where c is the number of classes, $p(i|t)$ denotes the fraction of observations that belong to class i at a given node t. The degree of impurity of the parent node and child nodes can be compared to determine the performance of a test condition. The gain term, Δ in Equation 2.8, can be used to determine the goodness of a split [7].

$$\Delta = I(parent) - \sum_{j=1}^{k} \frac{N(v_j)}{N} I(v_j) \tag{2.8}$$

where *I* is the impurity level of a given node, *N* is the total number of observations at the parent node, *k* is the number of attribute values, and $N(v_j)$ is the number of observations related to the child node, v_j. Maximization of the gain equals to minimization of the impurity measures of the child nodes because *I(parent)* is the same for all test conditions [7].

After the construction of a decision tree, pruning step can be performed in order to reduce its size. Tree pruning improves the generalization performance of the decision tree. Too large decision trees are not preferred because of overfitting problem. Therefore different pruning levels are applied to decision tree to understand the effect of overfitting and underfitting. When the size of a tree is too small, training and test error rate of the model are large because of the model underfitting. If a model has continued to learn the structure of the data, underfitting occurs so the model performs poorly on training and test set. When the number of nodes in a decision tree increases, training error rate decreases continuously but test error rate decreases and then rises again because of the model overfitting. This situation is shown in Figure 2.2 [7].

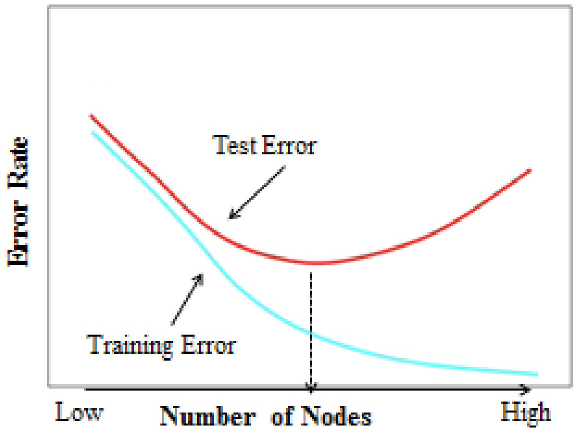

Figure 2.2. Error rates as a function of tree depth [9].

Data set can be randomly divided into two sets: one set to be used for training and constructing the decision tree model while the other to be used for testing the generalization ability of the model. In order to determine the performance of a classification model, the counts of test records correctly and incorrectly predicted by the model can be written in a table known as confusion matrix. Although a confusion matrix gives the information about the performance of a model, indicating the performance of a model with a number is more beneficial to make comparison with the performance of other models. The performance of a model can be expressed in terms of its accuracy [Eq. (2.9)] or error rate [Eq. (2.10)], obviously. The highest accuracy or the lowest error rate is desired to find the best model [7]. In this thesis, error rate was used for the performance evaluation of decision trees but accuracy was also calculated. Apart from these, confusion matrices for training and testing were formed using the results of optimum trees.

$$Accuracy = \frac{Number\ of\ correct\ predictions}{Total\ number\ of\ predictions} \tag{2.9}$$

$$Error\ rate = \frac{Number\ of\ wrong\ predictions}{Total\ number\ of\ predictions} \tag{2.10}$$

2.3.2. Prediction by Artificial Neural Networks

Artificial neural networks (ANN) were inspired by biological neural systems of human brain consisting of neurons and synapses [7]. Neural networks are used both for classification and regression because it is a nonparametric method [21]. The Kohonen network, which is an unsupervised learning network, is used for clustering while the multilayer perceptron and the radial basis function, which are supervised learning networks, are used for prediction of one or more dependent variables. Neural networks are used widely because of their success in modeling for even very complex functions. The ability to deal with nonlinear relations among variables is a major benefit of neural networks. However, black box nature of the networks, too many parameters to adjust, the amount of computing power required and generally the risks of overfitting are some of the main disadvantages of ANN [9].

A simple neural network topology is known as a perceptron (Figure 2.3). The perceptron consists of input nodes that represent the attributes and an output node that represents the model output. Each input node is connected to the output node via the weighted link [7]. The output includes all the units of the input layer with a combination and transfer (or activation) function [9]. The bias, denoted by b_k in Figure 2.3, increases or decreases the net input of the activation function depending on whether it is positive or negative [22]. A perceptron cannot find the right solution for nonlinearly separable data [7].

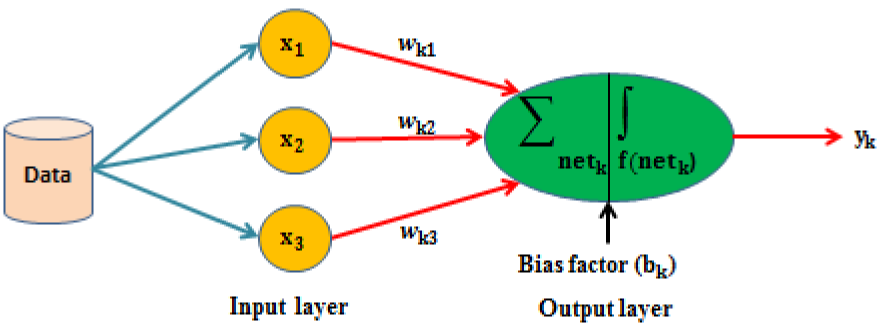

Figure 2.3. A simple neural network (a perceptron) [22].

Model of an artificial neuron is formalized using the following notation. There can be several inputs x_i, i=1,2,3,...,m. Each input x_i is multiplied by the corresponding weight

w_{ki} where k is the index of a given neuron in an ANN. The weighted sum of products $x_i w_{ki}$, for i=1,...,m is usually denoted as *net* [Eq. (2.11)] [22].

$$net_k = x_0 w_{k0} + x_1 w_{k1} + x_2 w_{k2} + \cdots + x_m w_{km} = \sum_{i=0}^{m} x_i w_{ki} \tag{2.11}$$

where $w_{k0}=b_k$ and default input $x_0=1$. Finally, transfer function (f), shown in Equation 2.12, is applied to net_k value to determine the output y_k. Sign, linear, sigmoid and tangent hyperbolic functions are some of the examples of activation functions. The output of an ANN is generally nonlinear function due to the preferred activation functions such as sigmoid or tanh function, ranging from -1 to +1 instead of 0 to +1. The comparison of the predicted output with the target value can be done by calculating sum of square error [Eq. (2.13)]. The basic model for one node can be extended for highly connected networks of artificial neurons [22].

$$y_k = f(net_k) \tag{2.12}$$

$$E(w) = \frac{1}{2}\sum_{i=1}^{N}(target - predicted)^2 \tag{2.13}$$

where N is the number of observation.

One or more hidden layers between the input and output layers can be added to the network in order to increase prediction performance of a model. The resulting structure is known as a multilayer neural network. It is generally used for complex non-linear models by extracting more features from the input patterns due to hidden nodes [9]. The only difference between a multilayer perceptron and a perceptron is that the output is a nonlinear function of the input due to the nonlinear basis function in the hidden units [21]. Figure 2.4 shows the graph of a multilayered perceptron with two hidden layers and an output layer. The neuron in any layer of the network is connected to all the neurons in the previous layer so the network is fully connected. The direction of the data flow is from up to down. Multilayer perceptrons with the error backpropagation algorithm have been used successfully to solve difficult problems [22].

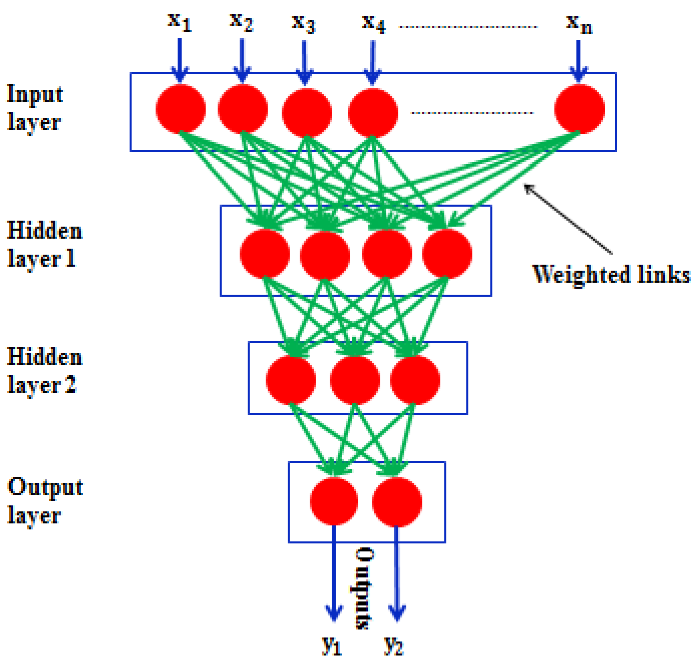

Figure 2.4. Example of a multilayer feed-forward artificial neural network [7].

The main aim of the ANN learning algorithm is to adjust a set of weights, w, that minimizes the total sum of squared errors [Eq. (2.13)]. The sum of squared error depends on w because the predicted value is a function of the weights assigned to the hidden and output nodes [7]. There are many algorithms to improve the prediction ability of the model. Gradient back-propagation algorithm is one of them, but there are more effective algorithms such as the Levenberg-Marquardt, quasi-Newton, conjugate gradient, quick propagation, and genetic algorithms [9]. Levenberg-Marquardt algorithm converges more quickly and provides a better solution than the gradient back-propagation algorithm. However, it is used for only a single output unit and it uses a large amount of computer memory [9].

The back-propagation algorithm, a gradient descent algorithm, is the oldest and widely used method for big data size [9]. This algorithm is based on the error-correction learning rule [22]. There are two phases in each iteration of the algorithm: the forward phase and the backward phase. In the forward phase, the weights obtained from the previous iteration are used to calculate the output value of each neuron in the network. Outputs of the neurons at level (k+1) are computed after outputs of the neurons at level k are computed. During this phase, the synaptic weights of the network are all fixed. In the backward phase, the weight update formula is applied in the reverse direction. The weights at level (k+1) are updated before the weights at level k are updated [7]. The synaptic weights are adjusted in accordance with an error-correction rule to make the response of the network closer to the desired value [22]. The weight update rules are given in the following equations:

$$w_{new} = w_{old} + \eta \frac{\partial E}{\partial w} \tag{2.14}$$

$$w_{ji,new} = w_{ji,old} + \Delta w_{ji} \tag{2.15}$$

$$\Delta w_{ji} = \eta . \delta_j . x_i = \text{Learning factor.(Desired output-Actual output).Input} \tag{2.16}$$

$$\delta_j = output_j\left(1 - output_j\right)\left(actual_j - output_j\right) \quad \text{for output layer nodes} \tag{2.17}$$

$$\delta_j = output_j\left(1 - output_j\right)\sum\left(w_{ji} . \delta_j\right) \quad \text{for hidden layer nodes} \tag{2.18}$$

$$\Delta w_{ji}(n+1) = \eta . \delta_j(n+1) . x_i(n+1) + \alpha . \Delta w_{ji}(n) \tag{2.19}$$

where η is the learning rate, x_i is the signal coming to the neuron, δ_j local gradient, $\sum\left(w_{ji} . \delta_j\right)$ is the accumulated backpropagated error from output units to the hidden units, α is a momentum constant [22]. Learning factor, η, determines the magnitude of change to be made in the weights during learning. $0.0 \le \eta \le 1.0$ but η is generally taken less than 0.2. The effect of the momentum can be seen at each parameter update [21]. Successive Δw_{ji} values can be so different that large oscillations may occur but the movement should be continued without being trapped by local minima to reach the global minima and to achieve convergence [9]. $0.0 \le \alpha \le 1.0$ but α is generally taken between 0.5 and 1.0 [21].

In a back-propagation network, a single hidden layer should be preferred to increase the robustness of the network. Instead of adding more hidden layers between input and output layers, modification of the other model parameters such as iteration, updating the initial weights or reprocessing the input data should be considered to improve the performance of the model. A network with m input units, a single hidden layer with p units and k output units has p(m+1) weights. Overcomplex model memorizes the noise in the training set and does not generalize to the validation set [9]. When training is continued too long, the error on the training set decreases continuously but the error on the validation set begins to increase beyond a certain point. While training continues, almost all weights are updated away from 0. Learning should be stopped early to prevent overtraining problem. The best way to determine the optimal point to stop training and the number of hidden units is to measure the error rate on the test sample, and stopping the increase in hidden units and epochs until this rate reaches a minimum value to avoid overfitting [21].

Generally, in the implementation of a neural network for prediction, following steps can be applied: (i) analyzing the structure of the input and output data, (ii) normalization of the data set depending on the limits of the transfer function used in the model, (iii) building of a suitable network structure, (iv) learning, (v) testing, (vi) model application, (vii) denormalization of the output data [9].

3. EXPERIMENTAL DATA AND COMPUTATIONAL DETAILS

3.1. Experimental Data

The database was constructed by extracting the experimental data on dry reforming of methane from published articles in American Chemical Society (ACS), Science Direct and Wiley between 2005 and 2014. The annual numbers of papers related to DRM is presented in Figure 3.1. This figure was drawn using the databases of Web of Science.

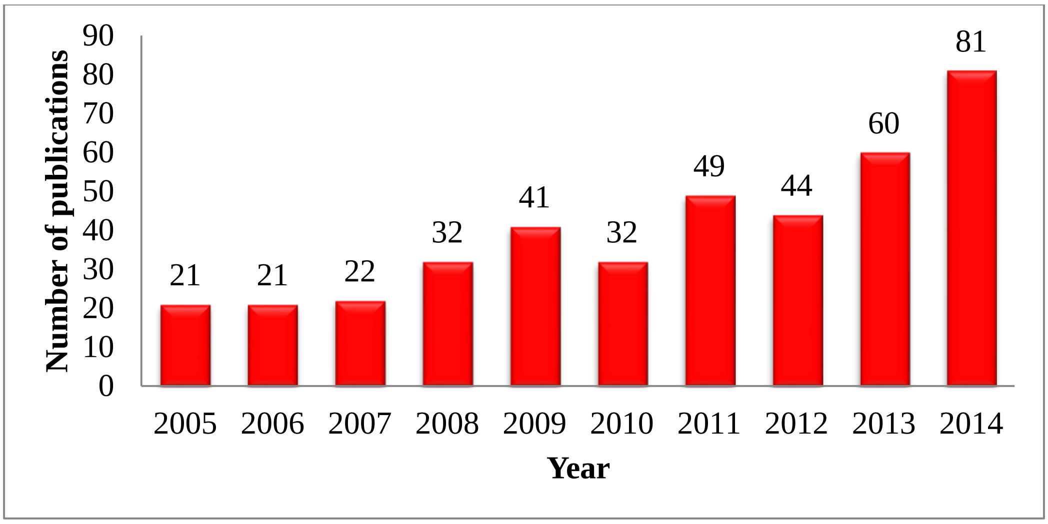

Figure 3.1. Number of publications related to DRM.

403 research publications were reviewed during the construction of the database but 105 articles with 6065 instances were used to construct the total data set because remaining papers were not suitable to extract data. However, 4 papers had to be excluded from the data set because these papers were unique to their study in terms of variables and outputs. During the collection of the data points, variables affecting the activity and the stability of DRM reaction were determined. These variables were metal types and loading, catalyst preparation techniques, calcination and reduction conditions, support type and loading and operating conditions. The final database consisted of 5521 experimental data with 63 input variables and 3 outputs. The details of the experimental data extracted from 101 published papers in the literature are presented in the following tables.

The total data set contained twenty types of metals that were continuous attributes. Nickel was the most commonly used base metal in published papers because of its lower cost and wide availability. Co was another commonly preferred non-noble base metal after Ni. Addition of small amount of second metals into Ni- or Co- based catalysts were commonly used methods to increase activity and stability of catalysts. Ba, Ca, Cu, Sr and Y were only used as promoters. Some noble metals such as Pt, Rh and Ru were used as base metals, second metals or promoters in the papers. In order to prevent the complexity of the data set, all metals were combined under the variable of metal types. Metal types and the range of metal types loading together with the number of data points are presented in Table 3.1.

Table 3.1. Metal types used as active metals or promoters for DRM reaction.

Variable Group	**Input Variable**	**Range (wt. %)**	**Data Number**
Metals used as active metals or promoters	Au	0-0.20	30
	Ba	0-2.69	20
	Ca	0-5.00	81
	Ce	0-15.00	262
	Co	0-30.00	718
	Cu	0-5.00	5
	Ir	0-5.00	40
	K	0-5.00	270
	La	0-14.45	351
	Li	0-0.50	12
	Mg	0-2.00	91
	Mn	0-5.00	27
	Ni	0-30.00	4223
	Pd	0-5.00	79
	Pt	0-5.00	738
	Rh	0-7.25	156
	Ru	0-5.00	189
	Sr	0-2.25	94
	Y	0-9.00	10
	Zr	0-11.10	44

Six different catalyst preparation techniques as categorical attributes were studied in the published papers for DRM reaction. These were Co-impregnation (CI), Co-precipitation (CP), Incipient to wetness impregnation (IWI), Sol-gel (SG), Sequential impregnation (SI) and Wet impregnation (WI). The most commonly used preparation method in DRM was wet impregnation. Catalyst preparation techniques together with the number of data points are shown in Figure 3.2.

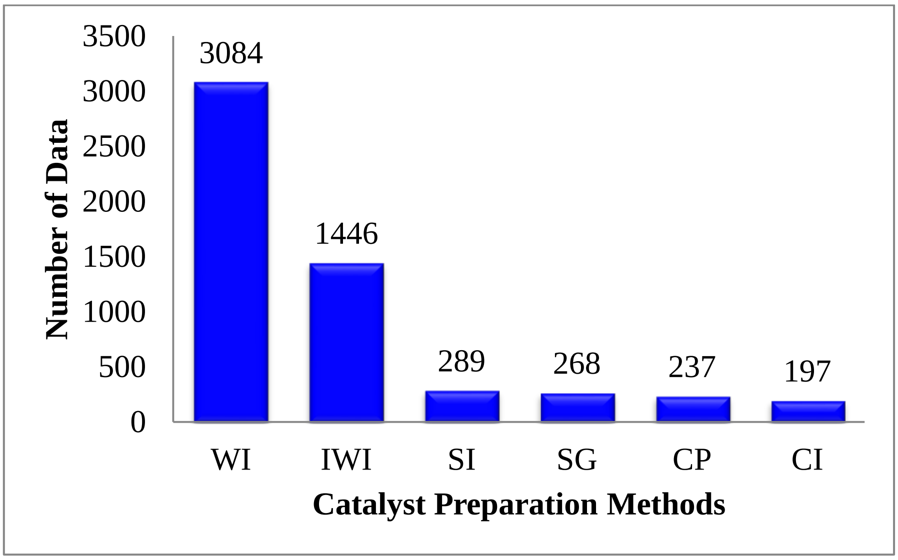

Figure 3.2. Catalyst preparation methods for DRM reaction.

Calcination step can be carried out after the preparation of catalysts. The ranges of calcination temperature and time are presented in Table 3.2. Calcination temperature and time were taken as continuous attributes. If catalysts were not calcined, the calcination temperature and time were taken as 25°C and 0 hour, respectively.

Table 3.2. Calcination conditions for DRM reaction.

Variable Group	**Input Variable**	**Range**
Calcination Conditions	Calcination Temperature (°C)	25-900
	Calcination Time (h)	0-12

After the calcination of the catalyst, in order to increase the activity of the catalyst, reduction can be carried out in pure H_2 or mixture of H_2 with other gases such as Ar, N_2 or He. However, only vol. %H_2 was taken as input variable because volumetric percentage of H_2 affected the performance of catalysts and other gases were only used as inert gases.

Reduction temperature, time and vol. %H_2 were taken as continuous attributes. If catalysts were not reduced, the reduction temperature, time and vol. %H_2 were taken as 0°C, 0 hour and 0 vol. %, respectively. The ranges of reduction temperature, time and volumetric percentage of H_2 are presented in Table 3.3.

Table 3.3. Reduction conditions for DRM.

Variable Group	**Input Variable**	**Range**
Reduction Conditions	Reduction Temperature (°C)	0-850
	Reduction Time (h)	0-10
	H_2 (vol. %)	0-100 %

Support types used in the catalysts for DRM reaction are presented in Table 3.4. The total data set contained 24 types of metals that were continuous attributes. Pure supports were labeled as 1 and mixed or modified supports were indicated with their weight percentages out of 1. γ-Al_2O_3 was the most commonly used support in the papers because of its availability and mild acidity. ZrO_2 was used as another prominent support because of its redox behavior, surface acidity, reducibility and higher thermal stability.

Table 3.4. Support types for DRM reaction.

Variable Group	Input Variable	Range (wt. % out of 1)	Data Number
Support	BaO	0-0.03	16
	$BaTiO_3$	0-1	12
	CaO	0-0.49	247
	CeO_2	0-1	571
	H-ZSM-5	0-1	12
	La_2O_3	0-1	141
	MCM-41	0-1	159
	Meso-Al_2O_3	0-1	75
	Meso-ZrO_2	0-1	284
	$MgAl_2O_4$	0-1	330
	MgO	0-1	446
	MnO	0-0.15	48
	Nano-MgO	0-1	514
	PrO_2	0-0.20	80
	SBA-15	0-1	197
	Si_3N_4	0-1	52
	SiO_2	0-1	408
	TiO_2	0-1	282
	V_2O_5	0-0.10	28
	Y_2O_3	0-0.20	108
	ZrO_2	0-1	753
	ZSM-5	0-1	198
	α- Al_2O_3	0-1	120
	γ- Al_2O_3	0-1	2132

Reaction temperature, feed compositions consisting of vol. %CH_4, vol. %CO_2, vol. %Ar, vol. %He and vol. %N_2, W/F and time on stream were taken as operating variables for DRM reaction. These features were continuous and presented in Table 3.5. Pressure was not considered as an input variable because all the experiments were performed at atmospheric pressure. The time on stream was assumed to be 60 minutes for the papers in which the value of this variable was not reported. Reactor types used for DRM reaction were mainly similar (fixed bed) so the reactor type was not used as a variable.

Table 3.5. Operating conditions for DRM reaction.

Variable Group	**Input Variable**	**Range**
Operating Conditions	Temperature (°C)	350-900
	CH_4 (vol. %)	10-83.33
	CO_2 (vol. %)	10-83.33
	Ar (vol. %)	0-80
	He (vol. %)	0-80
	N_2 (vol. %)	0-75
	W/F (mgmin/ml)	0.15-88.24
	Time on Stream (TOS) (min)	0-7800

Finally, the products of dry reforming of methane reaction are H_2 and CO. Although the outputs that were extracted from papers were CH_4 conversion, CO_2 conversion and H_2/CO ratio, the conversion of CO_2 and H_2/CO were not as complete as the CH_4 conversion throughout the entire data set so only the conversion of CH_4 was used as the dependent variable. Output variables are presented in Table 3.6 together with the number of data points. Calculation of the CH_4 and CO_2 conversion and H_2/CO ratio are given in Equation 3.1, Equation 3.2 and Equation 3.3, respectively. In this thesis, CH_4 conversion and H_2/CO values were used as outputs for decision tree analyses and the former was used as output for neural network analyses.

Table 3.6. Output variables for DRM reaction.

Outputs	**Range**	**Number of Data**
CH_4 Conversion (%)	0-100	5521
CO_2 Conversion (%)	0-100	3930
H_2/CO Ratio	0-3.21	2323

$$X_{CH_4} = \frac{(F_{CH_4,in} - F_{CH_4,out})}{F_{CH_4,in}} \times 100 \tag{3.1}$$

$$X_{CO_2} = \frac{(F_{CO_2,in} - F_{CO_2,out})}{F_{CO_2,in}} \times 100 \tag{3.2}$$

$$\frac{H_2}{CO} = \frac{mole\ of\ H_2\ produced}{mole\ of\ CO\ produced} \tag{3.3}$$

3.2. Computational Details

In this study, MATLAB R2013b was used for computational work. CH_4 conversion for DRM reaction was used as output variable with 5521 instances. Two data mining techniques that are decision trees and artificial neural networks were applied to the total data set to extract knowledge for:

(i) Determining conditions and rules for higher catalytic performance
(ii) Determining the significance of input variables
(iii) Predicting the outcome of unstudied conditions without doing an experiment

3.2.1. Decision Tree Modeling

Decision tree classification was used to understand the conditions and rules that led to higher CH_4 conversion. Firstly, experimental data was called from excel file and saved in the workspace of the MATLAB. The output that was CH_4 conversion was converted into classes. Determination of the class interval was done by considering test error rate of the entire tree, objective of the analyses and class balance. CH_4 conversion levels were described in three classes as 0-50, 50-75 and 75-100. The total data set was randomly divided into two sets. Two third of the total data was used as training and constructing the decision tree and one third of the total data was used as testing and evaluating its generalization ability. Gini's diversity index (default in MATLAB) was used to select optimal split for the decision tree. The total error rate of the entire tree should be minimized by trying several splits. Different splitmin values ranged from 25 to 300 with an increment of 25 were tried. Different levels of pruning were applied to the entire tree in order to prevent the complexity of the tree. When the tree becomes too large that means higher number of nodes, overfitting can occur and when the tree was too small that means smaller number of nodes, underfitting can occur. Therefore after the determination of the optimum splitmin value, training and testing error rate of the tree in different number of pruning levels as well as different number of nodes should be calculated in order to select the best tree with the smallest error rate for testing and the highest generalization ability. Finally, optimal tree was used for rule deduction and the confusion matrices of that tree were also formed to comprehend misclassification errors.

3.2.2. Artificial Neural Network Modeling

Various network topologies were investigated in order to determine the optimal one in terms of the highest coefficient of determination value and the lowest root mean square error (RMSE). Two back-propagation training algorithms including Levenberg-Marquardt (trainlm) and Bayesian Regularization (trainbr) were used with changes in the number of neurons and hidden layers with different transfer functions including the tangent sigmoid (tansig), log sigmoid (logsig) and linear function (purelin). In this thesis, one hidden layer produced better results than two hidden layers. Basic steps for designing ANN models were represented in Figure 3.3.

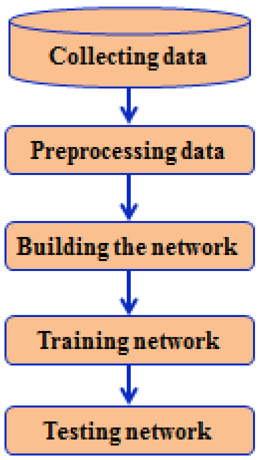

Figure 3.3. Basic steps for designing ANN models.

After the collection of data, three data preprocessing techniques that are filling/eliminating the missing value, normalization of data and randomization of data were applied to data set. 698 time on stream value could not be extracted from the papers in which these values were not reported. Therefore, these missing data were replaced by 60 min because initial activity measurement is generally conducted after 60 minutes. Also in some articles, gas hourly space velocity values (GHSV), which are highly significant for

DRM reaction, were reported while the others were reporting W/F (catalyst weight/flow rate) ratio. Therefore GHSV values (ml/hg$_{cat}$) were converted into W/F (mgmin/ml) in order to be able to express this attribute as a single variable. Normalization step was applied to the input and output data in accordance with the transfer function. The mapminmax function normalizes the data so that all data falls in the range [-1, +1]. The network output was transformed back into its original range because output of the network fell in the normalized range. Tansig was used as in the hidden layer as the activation function because of its suitability to our data set and it was shown in Figure 3.4. Training data was randomized using randperm function. This function returns a random permutation of the 5521 instances while keeping the input columns constant [23].

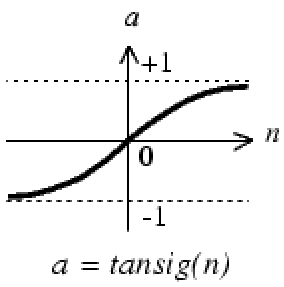

Figure 3.4. Tan-sigmoid transfer function [23].

'newff' function was used to create a feed-forward back-propagation network. This command automatically initializes the weights and biases. ANN models were trained by the Levenberg-Marquardt (trainlm) method, which is the fastest training function, based on gradient descent and Gauss-Newton iteration. Trainbr was used for testing. It is used for determining the optimal regularization parameters automatically. The regularization parameters depend on the unknown variances associated with specified distributions. The weights and biases can be considered as random variables. When trainbr function is used, the algorithm should be run until the effective number of parameters has converged. Trainbr usually works well with early stopping [23]. Mean square error (MSE) was used as the performance function and tansig was used as transfer function. Each network topology was trained 10 times in order to eliminate the effects of random initialization of the neural network weights. Early stopping technique was used in order to prevent the model overfitting. Different number of neurons in one layer were tried [24].

Test data was used to determine the optimal neural network topology. The root mean square error (RMSE) of testing was calculated applying the 4-fold cross validation technique. The entire database was randomly divided into 4 sets. 3 sets were used to train the network to predict the remaining one set. This procedure was repeated 4 times for 4 sets. The error between the predicted value and the target value of the corresponding experiment was calculated for each instance and the errors of the sets were combined. Finally, RMSE was calculated using the error values of 4 sets. Each fold in 4-fold cross validation was repeated ten times. The optimal neural network topology was determined by the RMSE value of the entire data set. Calculation of the RMSE is shown in Equation 3.4.

$$RMSE = \sqrt{\frac{1}{N} \times \sum_{i=1}^{N} (t_i - p_i)^2} \tag{3.4}$$

and where p_i is the predicted value, t_i is the target value and N is the number of experiments.

Apart from the calculation of the RMSE value, R squared (R^2), known as the coefficient of determination, was calculated in order to determine how well the model fits to the data. R^2 is a statistical measure of how close the target values to the predicted values. R^2, shown in Equation 3.5, takes the value between 0 and 1. If a model covered 100% of the variance, the predicted values were equal to the target values. Only R^2 value does not prove whether or not a model is sufficient so RMSE values were also calculated with the corresponding R^2 values.

$$R^2 = 1 - \frac{SS_{res}}{SS_{tot}} = 1 - \frac{\sum_{i=1}^{N}(t_i - p_i)^2}{\sum_{i=1}^{N}\left(t_i - t_{average}\right)^2} \quad where \quad t_{average} = \frac{\sum_{i=1}^{N} t_i}{N} \tag{3.5}$$

In order to try the performance of the optimal model on each paper, firstly total data set was separated in accordance with different experiments. One set of the experiments was removed from the data set. And then network was trained with the remaining experiments in order to predict the outputs of the removed experiments. This procedure was repeated for all (753 experiments) experiments. For each experiment RMSE and R^2 values were calculated. And then the predicted outputs of experiments and the target values of the corresponding experiments were combined in a matrix. In order to determine the performance of the model in a specified paper, the predicted value and the real value of the experiments related to a specified paper were extracted from the matrix to calculate the RMSE and R^2 value of the paper.

The change of root mean square error technique was used to find the significance of input variables. The procedure of the method was as follows: one of the input groups or input variables was removed from the data set, and then network was trained with the remaining input groups or variables. The RMSE value of the model calculated in the absence of this input group or variable was compared with the original RMSE calculated in the presence of all input variables. The difference was used as the significance of this input group [25].

4. RESULTS AND DISCUSSION

In this thesis, two data mining techniques that are decision trees and artificial neural networks were applied to the experimental data extracted from published papers in the literature. Therefore, Results and Discussion part is presented in two sections. First, decision tree analyses of experimental data are presented in six subsections: 'CH_4 conversion results of total data', 'CH_4 conversion results of Ni base data', 'CH_4 conversion results of Co base data', 'CH_4 conversion results of Pt base data', 'CH_4 conversion results of wet impregnation method data' and 'H_2/CO results of total data'. Ni, Co and Pt base data sets were generated using total data set because they were commonly studied metal types for DRM reaction in the literature. Wet impregnation was one of the most commonly used catalyst preparation techniques for DRM reaction so one data set was produced for this type of catalyst preparation method. In addition to these data sets, one data set was produced for the experiments having H_2/CO values as the outputs. Six decision trees were obtained using each type of data sets. The optimal decision trees were found by trying the different splitmin and prune values. The optimal trees with the lowest test error percentages and the highest generalization ability were selected. General knowledge and rules about each type of data sets were deduced from their corresponding trees. Second, the modeling results of the total data are discussed. The optimal neural network topology with the highest prediction ability was determined changing the number of neurons in each hidden layer, training and activation function. Each neural network was trained 10 times in order to eliminate the effects of the random initialization of the neural network weights. The optimal neural network topology was selected in accordance with the RMSE value of testing results. Finally, significance of the 63 input variables, prediction ability of the 753 experiments and 101 papers were analyzed using the optimal neural network topology.

4.1. Decision Tree Analysis for Knowledge Extraction

4.1.1. Analysis of CH_4 Conversion Results Using Entire Data Set

The total data including 5521 instances with 63 attributes were classified according to their CH_4 conversion levels as 0-50 consisting of 2197 data, 50-75 consisting of 1798 data and 75-100 consisting of 1526 data and they were divided randomly into two parts as training and testing sets. Two third of the total data including 3681 instances was used to construct the decision tree and to train it while the remaining one third of the total data including 1840 instances was used to test the generalization ability of the decision tree. The optimal decision tree was found by starting with a large tree and then 10 levels of pruning were applied to the fully grown tree until the minimum test error rate was found. When the size of the tree increased, training error decreased continuously but test error decreased first and then increased due to the model overfitting. The training and test error rates for various tree sizes having the splitmin value 150 were shown in Figure 4.1. The tree with the minimum test error percentages was found with 39 nodes corresponding to prune level 5, training and test errors of 21.1% and 21.5%, respectively. The optimal decision tree was shown in Figure 4.2.

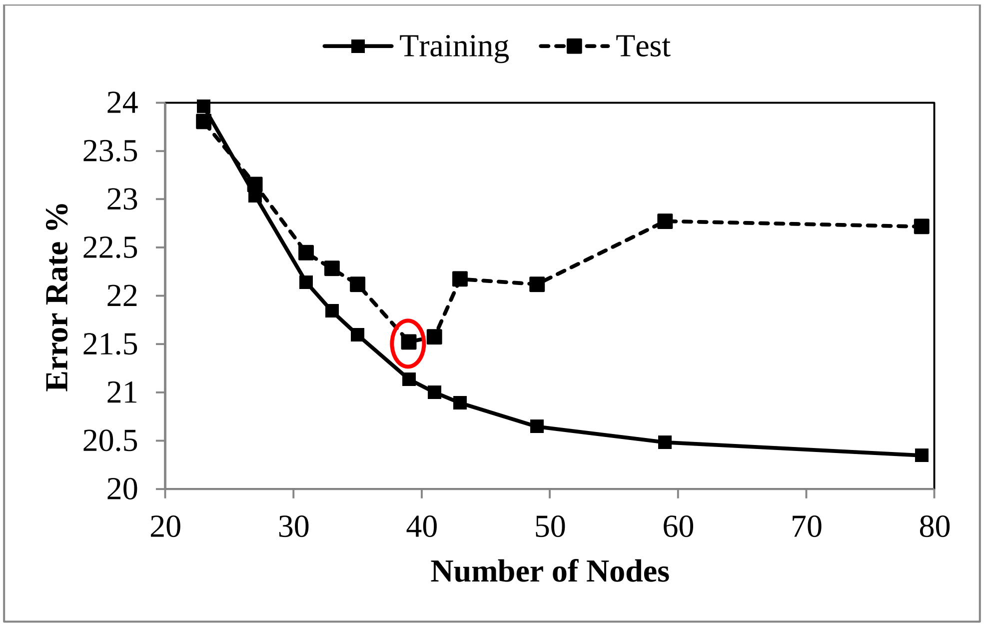

Figure 4.1. Training and test error rates of total data set.

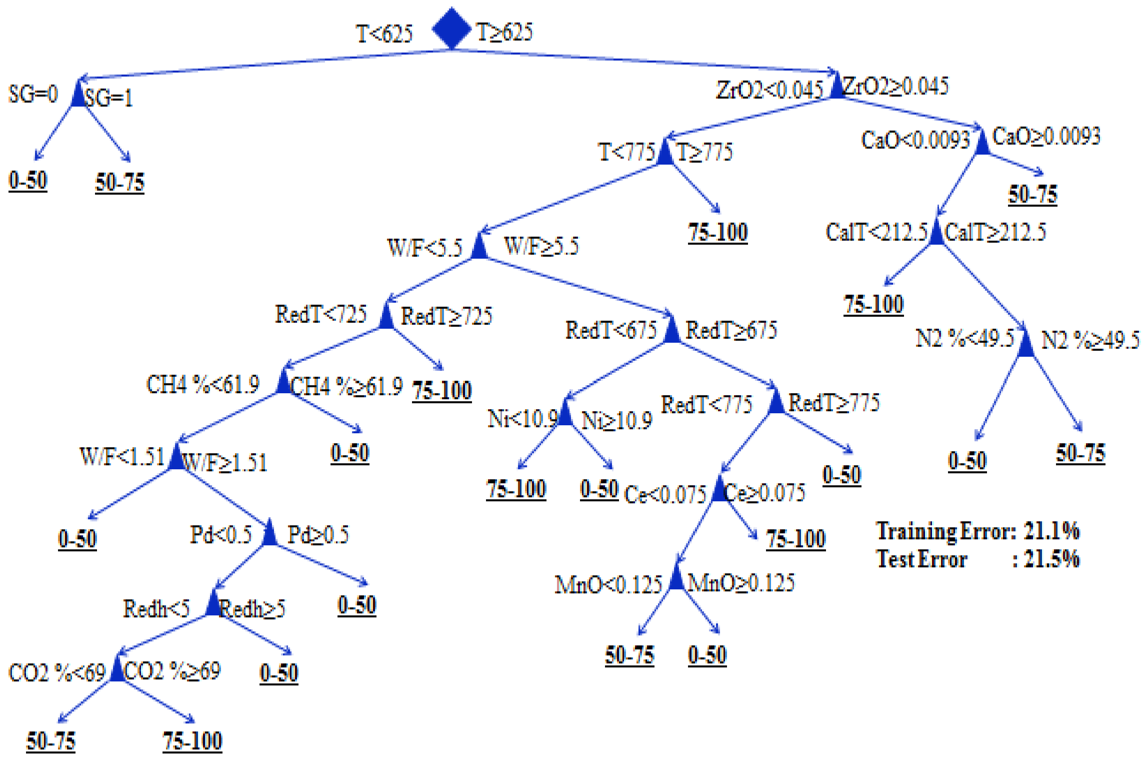

Figure 4.2. Optimal decision tree for total data.

Figure 4.2 reveals that the data were first divided at the top of the tree according to the reaction temperature indicating that this variable was the most significant factor determining the CH_4 conversion level. Temperatures that were lower than 625 °C led to lower CH_4 conversion while temperatures that were higher than 625 °C resulted in higher CH_4 conversion for some catalysts and operating conditions. This division was acceptable and consistent with the results of the experiments because of the highly endothermic nature of the DRM reaction. 625 °C was the split value calculated by the learning algorithm of the tree and it is not an exact physical limit. The same is valid for the values of all the other variables so they should be thought as some empirical approximations. The second decision point was the amount of ZrO_2 support. Mixed oxide supports were commonly used for DRM reaction. In the study of Pompeo *et al*. (2009), they investigated the addition of small amounts of CeO_2 and ZrO_2 to α-Al_2O_3 and they found that this mixed oxide support improved the Ni dispersion and the metal particle reducibility [26]. If the amount of ZrO_2 was higher than 0.045, that is equal to 4.5 wt.% of support part of the catalyst, the desired conversion level was possible only if the amount of CaO in the support and the calcination temperature of the catalyst were lower than 0.93% and 212.5 °C, respectively. If the amount of ZrO_2 was lower than 0.045, the desired conversion level was possible only if the reaction temperature was higher than 775 °C, otherwise W/F, reduction temperature and time, the amount of Ce, Ni and Pd metals in the catalysts, CH_4 and CO_2 volumetric feed percentages in the feed stream became significant to reach high conversion levels.

The rules deduced from the above tree were presented in Table 4.1. The shaded regions in the below table show the conditions required for more than 75% CH_4 conversion. There could be six options to reach the desirable conversion levels. Left hand side of the below table showed the most general conditions and moving along the right hand side of the table resulted in more specific conditions. Rule does not imply any theoretical rule. It describes the statement explaining the experimental pattern derived from the database.

Table 4.1. Rules for 75-100% CH_4 conversion for total data.

<table>
<tr><td rowspan="2">T<625</td><td colspan="9">Preparation Method: SG</td><td>50-75</td></tr>
<tr><td colspan="9">Preparation Method: IWI,WI,CI,CP,SI</td><td>0-50</td></tr>
<tr><td rowspan="18">T≥625</td><td rowspan="4">ZrO2≥0.045</td><td colspan="8">CaO≥0.0093</td><td>50-75</td></tr>
<tr><td rowspan="3">CaO<0.0093</td><td colspan="7">CalT<212.5</td><td>75-100</td></tr>
<tr><td rowspan="2">CalT≥212.5</td><td colspan="6">N2 %≥49.5</td><td>50-75</td></tr>
<tr><td colspan="6">N2 %<49.5</td><td>0-50</td></tr>
<tr><td rowspan="14">ZrO2<0.045</td><td colspan="8">T≥775</td><td>75-100</td></tr>
<tr><td rowspan="13">T<775</td><td rowspan="6">W/F≥5.5</td><td rowspan="4">RedT≥675</td><td colspan="5">RedT≥775</td><td>0-50</td></tr>
<tr><td rowspan="3">RedT<775</td><td colspan="4">Ce≥0.075</td><td>75-100</td></tr>
<tr><td rowspan="2">Ce<0.075</td><td colspan="3">MnO≥0.125</td><td>0-50</td></tr>
<tr><td colspan="3">MnO<0.125</td><td>50-75</td></tr>
<tr><td rowspan="2">RedT<675</td><td colspan="5">Ni≥10.9</td><td>0-50</td></tr>
<tr><td colspan="5">Ni<10.9</td><td>75-100</td></tr>
<tr><td rowspan="7">W/F<5.5</td><td colspan="6">RedT≥725</td><td>75-100</td></tr>
<tr><td rowspan="6">RedT<725</td><td colspan="5">CH4 %≥61.9</td><td>0-50</td></tr>
<tr><td rowspan="5">CH4 %<61.9</td><td rowspan="4">W/F≥1.51</td><td colspan="3">Pd≥0.5</td><td>0-50</td></tr>
<tr><td rowspan="3">Pd<0.5</td><td colspan="2">Redh≥5</td><td>0-50</td></tr>
<tr><td rowspan="2">Redh<5</td><td>CO2 %≥69</td><td>75-100</td></tr>
<tr><td>CO2 %<69</td><td>50-75</td></tr>
<tr><td colspan="4">W/F<1.51</td><td>0-50</td></tr>
</table>

The distribution of training and testing errors among tree classes for the optimum (above) tree are presented in Table 4.2 and Table 4.3, respectively. Classification accuracy of training was 78.9%. Classification accuracy of testing (78.5%) can be considered as acceptable because 1445 data out of 1840, which were not seen by the model during training, were classified correctly. The prediction accuracies for the lowest and highest conversion classes are higher; it seems that the model predicts the extreme conditions better as expected. This is also valid for the analyses presented in the remaining part of the thesis. It should be also considered that the class size of tree is relatively small, and the accuracy will decline if the model forced to classify the results in narrower intervals.

Table 4.2. Classification accuracies of each class for training data of entire data set.

Experimental Data		**Predictions for Training**			
Conversion	Number of data	0-50	50-75	75-100	Classification Accuracy (%)
0-50	1459	**1233**	153	73	84.5
50-75	1206	190	**857**	159	71.1
75-100	1016	48	155	**813**	80.0

Table 4.3. Classification accuracies of each class for testing data of entire data set.

Experimental Data		**Predictions for Testing**			
Conversion	Number of data	0-50	50-75	75-100	Classification Accuracy (%)
0-50	738	**611**	86	41	82.8
50-75	592	103	**420**	69	70.9
75-100	510	16	80	**414**	81.2

4.1.2. Analysis of CH_4 Conversion Results Using Ni Base Data Set

The Ni base data including 3966 instances with 52 attributes were classified according to their CH_4 conversion levels as 0-50 consisting of 1258 data, 50-75 consisting of 1388 data and 75-100 consisting of 1320 data. 2644 instances were used as training and the remaining 1322 instances were used as testing set. The optimal decision tree was found by starting with a large tree and then 10 levels of pruning were applied to the fully grown tree until the minimum test error rate was found. The training and test error rates for various tree sizes having the splitmin value 125 were shown in Figure 4.3. The tree with the minimum test error percentages was found with 43 nodes, corresponding to prune level 6, training and test errors of 16.7% and 19.0%, respectively. The optimal decision tree was shown in Figure 4.4.

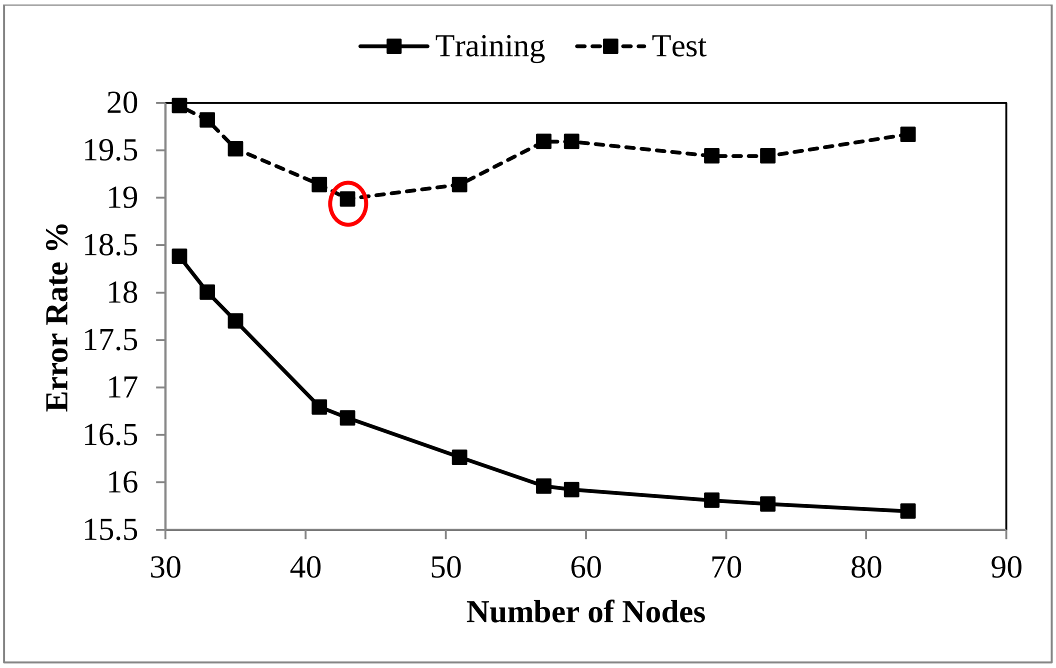

Figure 4.3. Training and test error rates of Ni base data set.

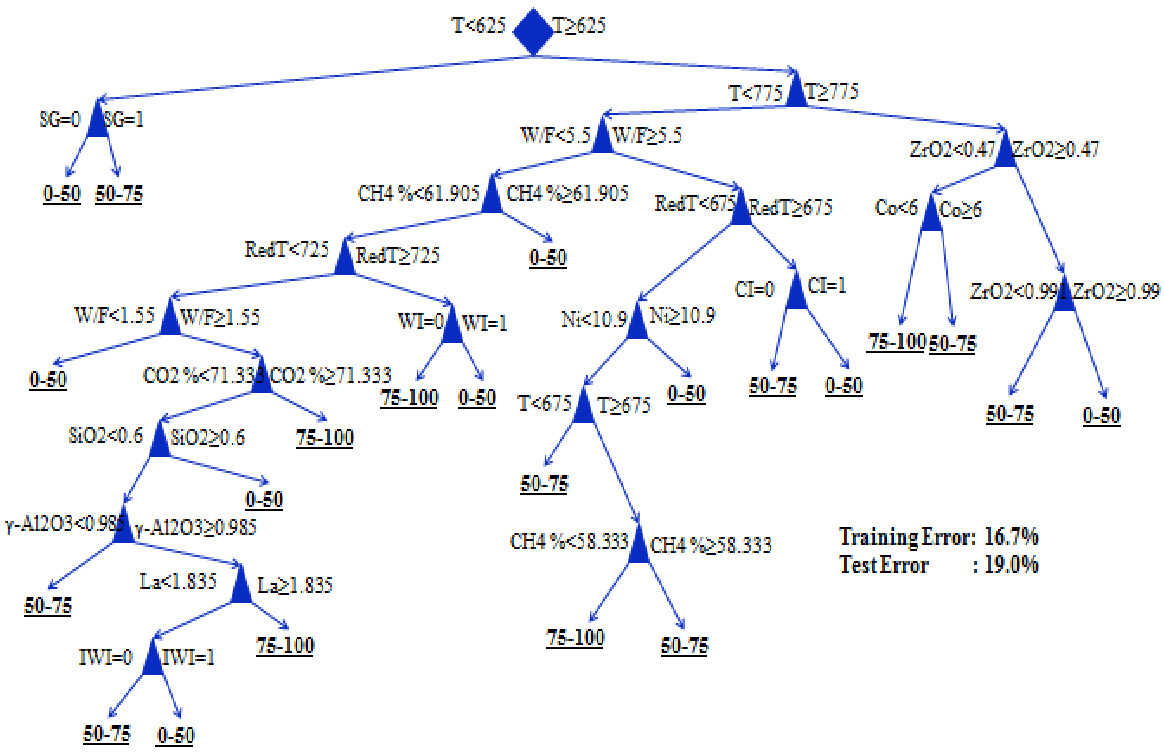

Figure 4.4. Optimal decision tree for Ni base data.

Similar to the tree of total data set, the first division was based on the reaction temperature. Ni was the most commonly used base metal for DRM reaction in literature and in total data set because of its availability and lower price. Ni was generally used with other metals to increase the activity and the stability of the catalyst. The decision tree showed that the highest CH_4 conversion level was not possible at the temperatures less than 625 °C. The second decision point was again reaction temperature. If the reaction temperature was higher than 775 °C, the desired conversion level was possible only if the amount of ZrO_2 in the support and the amount of Co metal in the catalyst were lower than 0.47 and 6, respectively. In the study of Luisetto *et al*. (2012), they found that bimetallic Ni-Co/CeO_2 catalyst was more active and selective than the monometallic Ni/CeO_2 catalyst because Co was highly effective to prevent carbon deposition [27]. The amount of Co and Ni in catalyst was also important because excessive amount of them could be resulted in deactivation of catalyst. If the reaction temperature was lower than 775 °C, the desired conversion level was possible with different four ways. In order to reach the desired conversion level, W/F, reduction temperature, the amount of Ni and La in catalyst, volumetric percentages of CH_4 and CO_2 in the feed stream and the amount of SiO_2 and γ-Al_2O_3 in the support were taken into consideration. The rules deduced from the tree were presented in Table 4.4.

Table 4.4. Rules for 75-100% CH_4 conversion for Ni base data.

T<625	Preparation Method=SG										50-75
	Preparation Method=IWI,WI,CI,CP,SI										0-50
T≥625	T≥775	ZrO2≥0.47	ZrO2≥0.991								0-50
			ZrO2<0.991								50-75
		ZrO2<0.47	Co≥6								50-75
			Co<6								75-100
	T<775	W/F≥5.5	redT≥675	CI							0-50
				IWI,WI,CP,SG,SI							50-75
			redT<675	Ni≥10.9							0-50
				Ni<10.9	T≥675	CH4%≥58.333					50-75
						CH4%<58.333					75-100
					T<675						50-75
		W/F<5.5	CH4%≥61.905								0-50
			CH4%<61.905	redT≥725	WI						0-50
					IWI,CI,CP,SI,SG						75-100
				redT<725	W/F≥1.55	CO2%≥71.333					75-100
						CO2%<71.333	SiO2≥0.6				0-50
							SiO2<0.6	γ-Al2O3≥0.985	La≥1.835		75-100
									La<1.835	IWI	0-50
										WI,CI,CP,SG,SI	50-75
								γ-Al2O3<0.985			50-75
					W/F<1.55						0-50

The confusion matrices belonging to the optimum Ni base tree for training and testing are presented in Table 4.5 and Table 4.6. Classification accuracies for both training and testing were higher than the entire tree as expected. Classification accuracy of testing (81%) can be considered as acceptable because 1071 data out of 1322 were classified correctly. The general characteristics of confusion matrices are quite similar to those obtained for the entire data.

Table 4.5. Classification accuracies of each class for training data of Ni base data set.

Experimental Data		**Predictions for Training**			
Conversion	Number of data	0-50	50-75	75-100	Classification Accuracy (%)
0-50	815	**713**	91	11	87.5
50-75	928	87	**739**	102	79.6
75-100	901	27	123	**751**	83.4

Table 4.6. Classification accuracies of each class for testing data of Ni base data set.

Experimental Data		**Predictions for Testing**			
Conversion	Number of data	0-50	50-75	75-100	Classification Accuracy (%)
0-50	443	**370**	64	9	83.5
50-75	460	70	**339**	51	73.7
75-100	419	11	46	**362**	86.4

4.1.3. Analysis of CH_4 Conversion Results Using Co Base Data Set

The Co base data including 718 instances with 39 attributes were classified according to their CH_4 conversion levels as 0-50 consisting of 358 data, 50-75 consisting of 143 data and 75-100 consisting of 217 data. 479 instances were used as training and the remaining 239 instances were used as testing set. The optimal decision tree was found by starting with a large tree and then 10 levels of pruning were applied to the fully grown tree until the minimum test error rate was found. The training and test error rates for various tree sizes having the splitmin value 25 were shown in Figure 4.5. The tree with the minimum test error percentages was found with 21 nodes, corresponding to prune level 3, training and test errors of 10.2% and 10.9%, respectively. The optimal decision tree was shown in Figure 4.6.

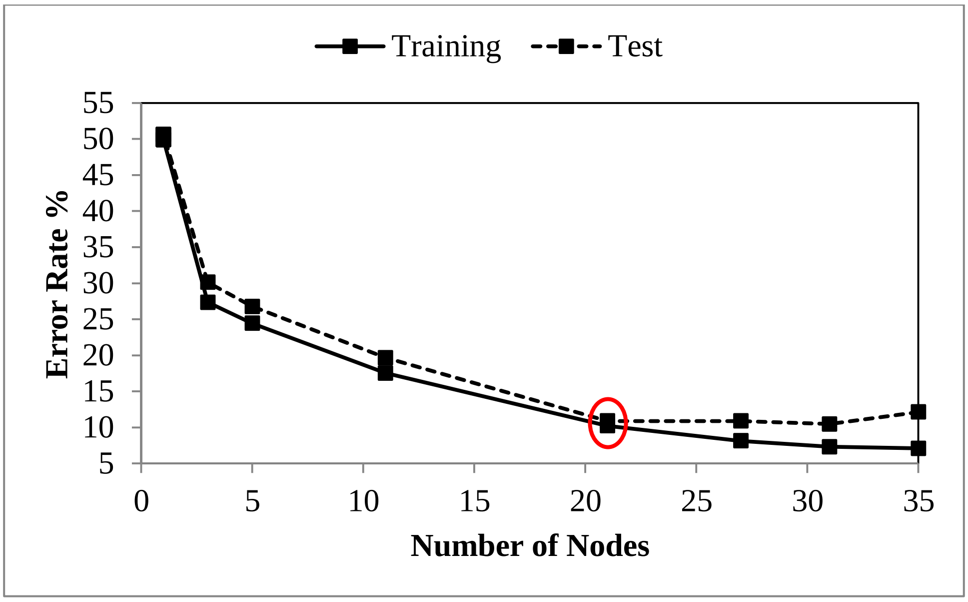

Figure 4.5. Training and test error rates of Co base data set.

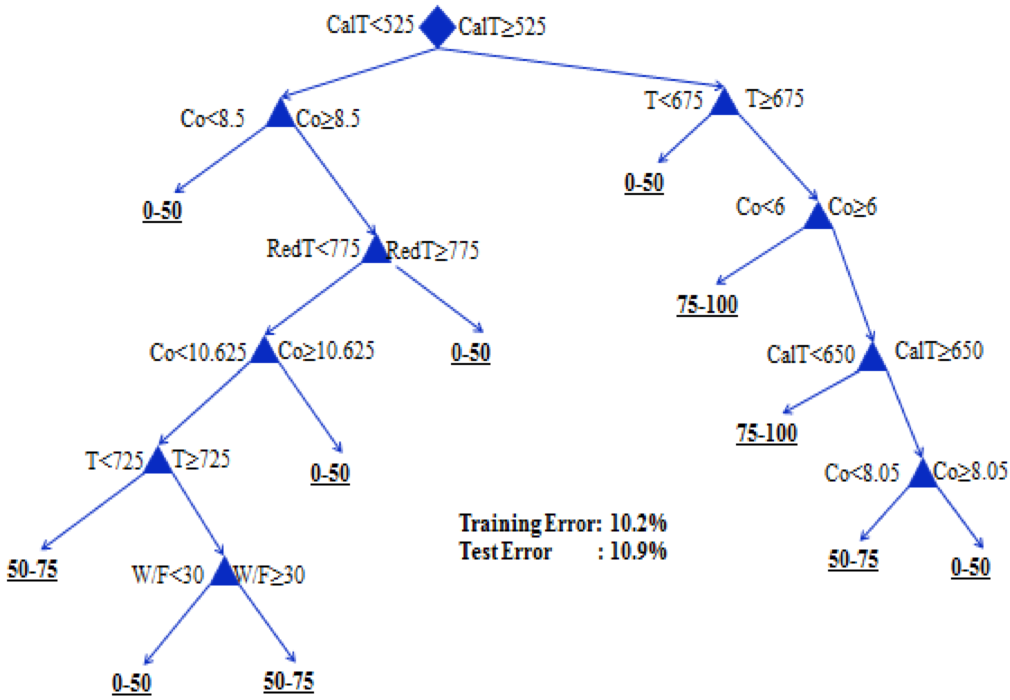

Figure 4.6. Optimal decision tree for Co base data.

Splitmin value for this data set was decreased to 25 because of a decrease in the number of instances. When splitmin value and prune level were decreased, test error rate was decreased but the complexity of trees increased so generalization ability of trees decreased. Therefore determining splitmin value was important to prevent deceptive results.

The Co base data were also divided according to calcination temperature first. The decision tree showed that the highest CH_4 conversion level was not possible if catalysts were calcined at the temperatures lower than 525 °C. Another division was done according to reaction temperature. If the reaction temperature was higher than 675 °C, the desired conversion level was possible with two ways. If the amount of Co metal in catalysts was lower than 6 wt.%, or if the amount of Co metal in catalysts that were calcined at the temperatures between 525 and 650 °C was higher than 6 wt.% , high conversion values could be reached. The rules deduced from the tree were presented in Table 4.7.

Table 4.7. Rules for 75-100%CH_4 conversion for Co base data.

<table>
<tr><td rowspan="6">CalT<525</td><td rowspan="5">Co≥8.5</td><td colspan="4">RedT≥775</td><td>0-50</td></tr>
<tr><td rowspan="4">RedT<775</td><td colspan="3">Co≥10.625</td><td>0-50</td></tr>
<tr><td rowspan="3">Co<10.625</td><td rowspan="2">T≥725</td><td>W/F≥30</td><td>50-75</td></tr>
<tr><td>W/F<30</td><td>0-50</td></tr>
<tr><td colspan="2">T<725</td><td>50-75</td></tr>
<tr><td colspan="5">Co<8.5</td><td>0-50</td></tr>
<tr><td rowspan="5">CalT≥525</td><td rowspan="4">T≥675</td><td rowspan="3">Co≥6</td><td rowspan="2">CalT≥650</td><td colspan="2">Co≥8.05</td><td>0-50</td></tr>
<tr><td colspan="2">Co<8.05</td><td>50-75</td></tr>
<tr><td colspan="3">CalT<650</td><td>75-100</td></tr>
<tr><td colspan="4">Co<6</td><td>75-100</td></tr>
<tr><td colspan="5">T<675</td><td>0-50</td></tr>
</table>

The confusion matrices belonging to optimum Co base tree for training and testing are presented in Table 4.8 and Table 4.9. 430 data out of 479 were classified correctly during training. The success of the tree was proved using the results of testing; 213 data out of 239 (89.1%) were classified correctly. Again tree placed the lower and higher conversion data with a remarkable accuracy while it was not that successful in the middle range.

Table 4.8. Classification accuracies of each class for training data of Co base data set.

Experimental Data		**Predictions for Training**			
Conversion	Number of data	0-50	50-75	75-100	Classification Accuracy (%)
0-50	240	**236**	4	0	98.3
50-75	93	35	**55**	3	59.1
75-100	146	4	3	**139**	95.2

Table 4.9. Classification accuracies of each class for testing data of Co base data set.

Experimental Data		**Predictions for Testing**			
Conversion	Number of data	0-50	50-75	75-100	Classification Accuracy (%)
0-50	118	**113**	4	1	95.8
50-75	50	16	**33**	1	66.0
75-100	71	1	3	**67**	94.4

4.1.4. Analysis of CH_4 Conversion Results Using Pt Base Data Set

The Pt base data including 738 instances with 34 attributes were classified according to their CH_4 conversion levels as 0-50 consisting of 507 data, 50-75 consisting of 155 data and 75-100 consisting of 76 data. 492 instances were used as training and the remaining 246 instances were used as testing set. The optimal decision tree was found by starting with a large tree and then 10 levels of pruning were applied to the fully grown tree until the minimum test error rate was found. The training and test error rates for various tree sizes having the splitmin value 25 were shown in Figure 4.7. The tree with the minimum test error percentages was found with 27 nodes, corresponding to prune level 2, training and test errors of 9.3% and 12.6%, respectively. The optimal decision tree was shown in Figure 4.8.

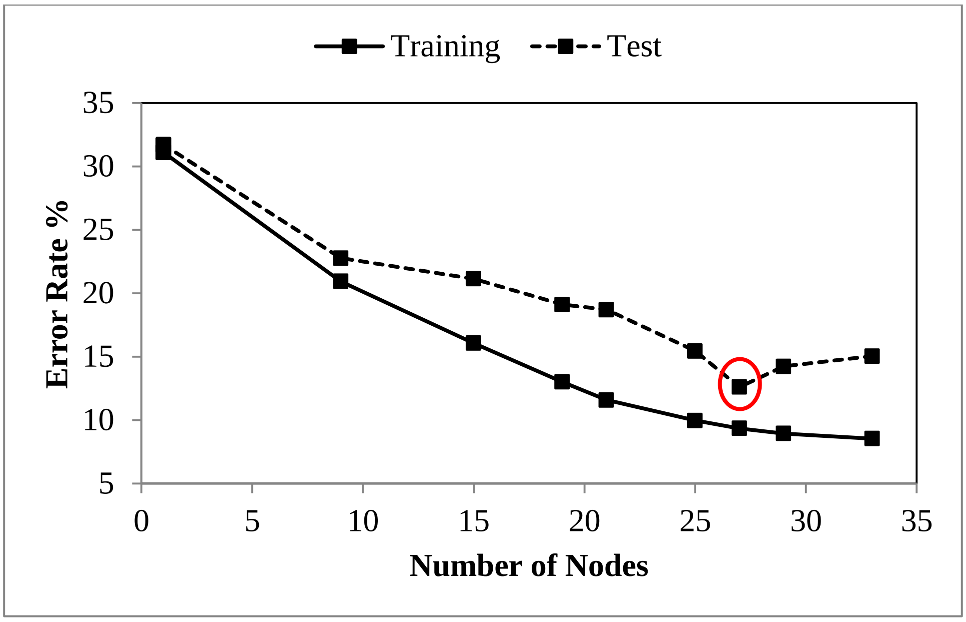

Figure 4.7. Training and test error rates of Pt base data set.

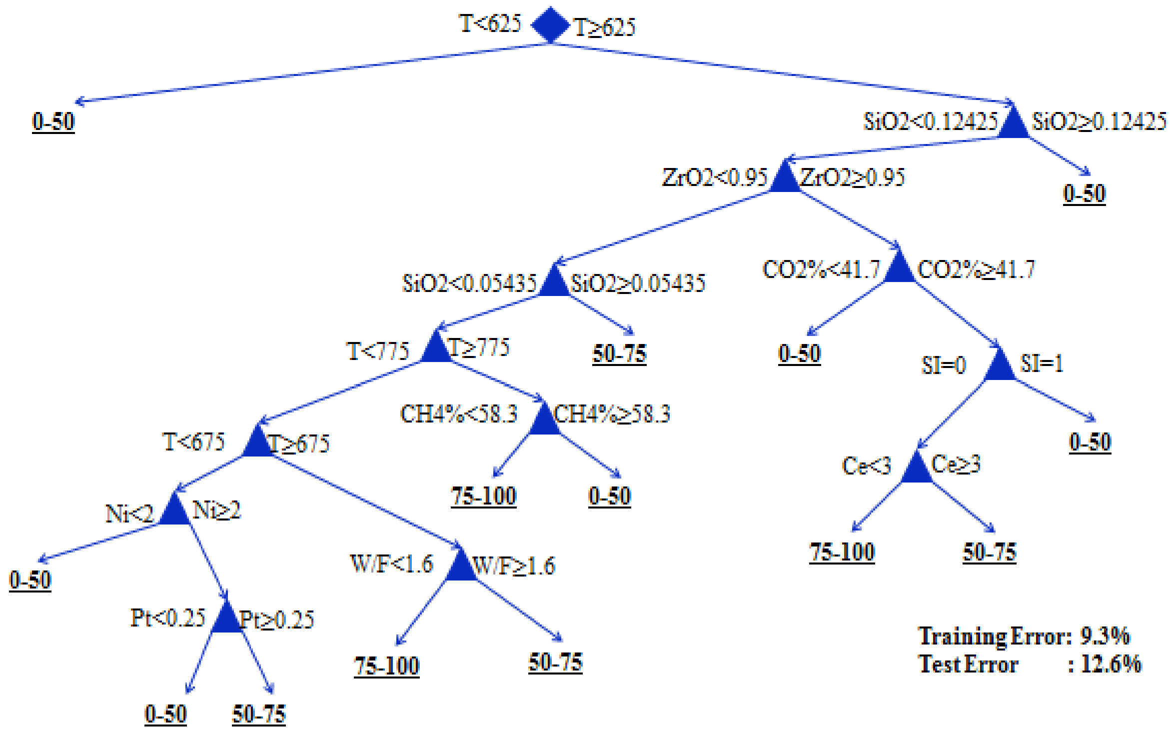

Figure 4.8. Optimal decision tree for Pt base data.

Similar to the tree of total and Ni base data sets, the first division was based on the reaction temperature. Pt was used as base metal and second active metal or promoter for DRM reaction. The decision tree showed that the highest CH_4 conversion level was not possible at the temperatures less than 625 °C. The second decision point was the amount of SiO_2 in support. The desired conversion level was possible only if the amount of SiO_2 in the support was lower than 0.12425. The other rules deduced from the tree were presented in Table 4.10.

Table 4.10. Rules for 75-100%CH_4 conversion for Pt base data.

<table>
<tr><td colspan="8">T<625</td><td>0-50</td></tr>
<tr><td rowspan="13">T≥625</td><td colspan="7">SiO2≥0.12425</td><td>0-50</td></tr>
<tr><td rowspan="12">SiO2<0.12425</td><td rowspan="4">ZrO2≥0.95</td><td rowspan="3">CO2%≥41.7</td><td colspan="4">SI</td><td>0-50</td></tr>
<tr><td rowspan="2">IWI,WI, CI</td><td colspan="3">Ce≥3</td><td>50-75</td></tr>
<tr><td colspan="3">Ce<3</td><td>75-100</td></tr>
<tr><td colspan="5">CO2%<41.7</td><td>0-50</td></tr>
<tr><td rowspan="8">ZrO2<0.95</td><td colspan="5">SiO2≥0.05435</td><td>50-75</td></tr>
<tr><td rowspan="7">SiO2<0.05435</td><td rowspan="2">T≥775</td><td colspan="3">CH4%≥58.3</td><td>0-50</td></tr>
<tr><td colspan="3">CH4%<58.3</td><td>75-100</td></tr>
<tr><td rowspan="5">T<775</td><td rowspan="2">T≥675</td><td colspan="2">W/F≥1.6</td><td>50-75</td></tr>
<tr><td colspan="2">W/F<1.6</td><td>75-100</td></tr>
<tr><td rowspan="3">T<675</td><td rowspan="2">Ni≥2</td><td>Pt≥0.25</td><td>50-75</td></tr>
<tr><td>Pt<0.25</td><td>0-50</td></tr>
<tr><td colspan="2">Ni<2</td><td>0-50</td></tr>
</table>

The confusion matrices belonging to optimum Pt base tree for training and testing are presented in Table 4.11 and Table 4.12. 446 data out of 492 were classified correctly during training. The success of the tree was proved using the results of testing; 215 data out of 246 (87.4%) were classified correctly.

Table 4.11. Classification accuracies of each class for training data of Pt base data set.

Experimental Data		**Predictions for Training**			
Conversion	Number of data	0-50	50-75	75-100	Classification Accuracy (%)
0-50	339	**324**	9	6	95.6
50-75	103	17	**78**	8	75.7
75-100	50	0	6	**44**	88.0

Table 4.12. Classification accuracies of each class for testing data of Pt base data set.

Experimental Data		**Predictions for Testing**			
Conversion	Number of data	0-50	50-75	75-100	Classification Accuracy (%)
0-50	168	**160**	6	2	95.2
50-75	52	13	**34**	5	65.4
75-100	26	0	5	**21**	80.8

4.1.5. Analysis of CH_4 Conversion Results Using Wet Impregnation Method Data Set

Wet impregnation method was commonly used catalyst preparation technique for DRM reaction. The wet impregnation base data including 3084 instances with 49 attributes were classified according to their CH_4 conversion levels as 0-50 consisting of 1100 data, 50-75 consisting of 1065 data and 75-100 consisting of 919 data. 2056 instances were used as training and the remaining 1028 instances were used as testing set. The optimal decision tree was found by starting with a large tree and then 10 levels of pruning were applied to the fully grown tree until the minimum test error rate was found. The training and test error rates for various tree sizes having the splitmin value 100 were shown in Figure 4.9. The tree with the minimum test error percentages was found with 39 nodes, corresponding to prune level 3, training and test errors of 13.6% and 15.1%, respectively. The optimal decision tree was shown in Figure 4.10.

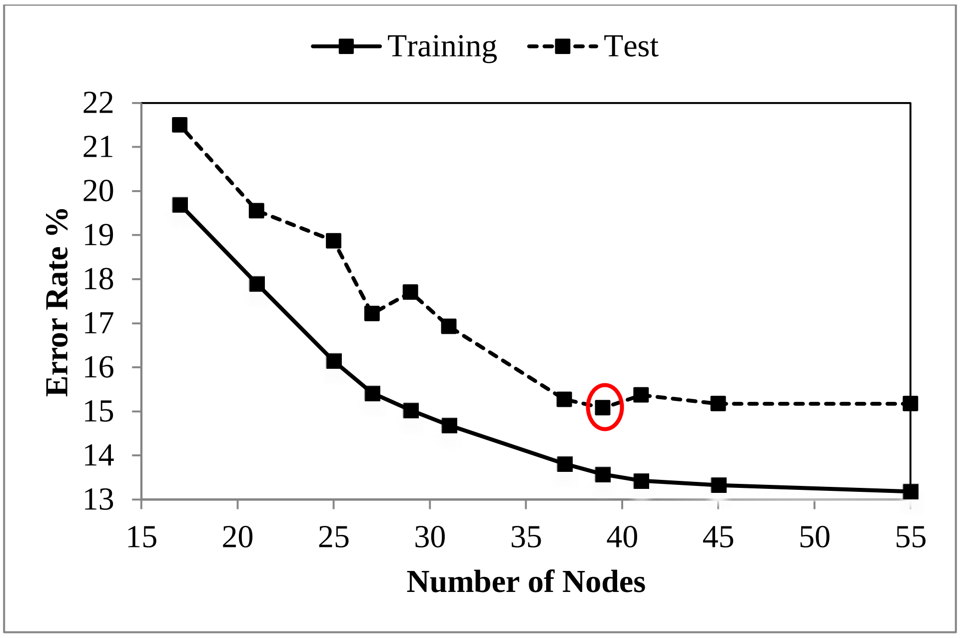

Figure 4.9. Training and test error rates of wet impregnation base data set.

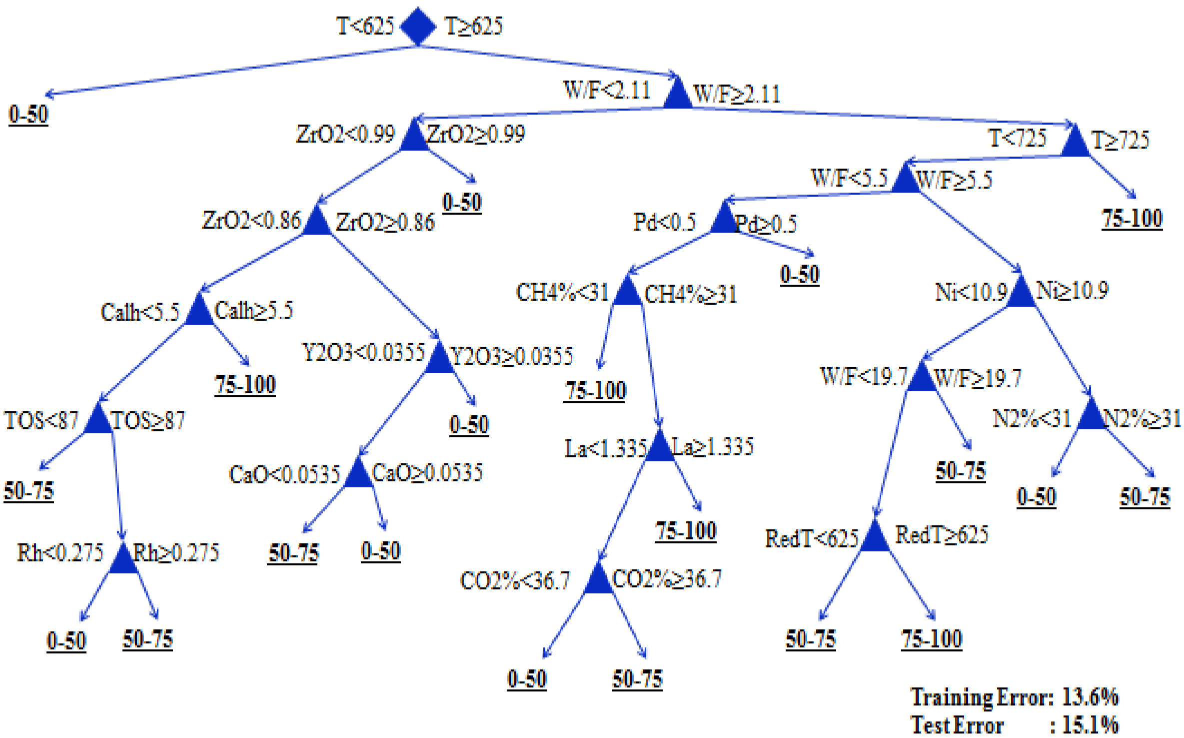

Figure 4.10. Optimal decision tree for wet impregnation base data.

Similar to the tree of total, Ni and Pt base data sets, the first division was done according to the reaction temperature. The decision tree showed that the highest CH_4 conversion level was not possible at the temperatures less than 625 °C. The second decision point was W/F value. If the W/F value was lower than 2.11, the desired conversion level was possible only if the amount of ZrO_2 in the support was lower than 0.86 and the calcination time of catalyst was higher than 5.5 hours. If the W/F value was higher than 2.11, the desired conversion level was possible with four different ways. In order to reach the desired conversion level, the reaction temperature, W/F, the amount of Ni, Pd and La in catalyst, reduction temperature and volumetric percentages of CH_4 in the feed stream were taken into consideration. The rules deduced from the tree were presented in Table 4.13.

Table 4.13. Rules for 75-100%CH_4 conversion for wet impregnation base data.

T<625								0-50
T≥625	W/F≥2.11	T≥725						75-100
		T<725	W/F≥5.5	Ni≥10.9	N2%≥31			50-75
					N2%<31			0-50
				Ni<10.9	W/F≥19.7			50-75
					W/F<19.7	RedT≥625		75-100
						RedT<625		50-75
			W/F<5.5	Pd≥0.5				0-50
				Pd<0.5	CH4%≥31	La≥1.335		75-100
						La<1.335	CO2%≥36.7	50-75
							CO2%<36.7	0-50
					CH4%<31			75-100
	W/F<2.11	ZrO2≥0.99						0-50
		ZrO2<0.99	ZrO2≥0.86	Y2O3≥0.0355				0-50
				Y2O3<0.0355	CaO≥0.0535			0-50
					CaO<0.0535			50-75
			ZrO2<0.86	Calh≥5.5				75-100
				Calh<5.5	TOS≥87	Rh≥0.275		50-75
						Rh<0.275		0-50
					TOS<87			50-75

The distribution of training and testing errors of the optimum tree belonging to wet impregnation base data set are presented in Table 4.14 and Table 4.15, respectively. Classification accuracy of training was 86.4%. Classification accuracy of testing (85%) can be considered as acceptable because 874 data out of 1028 were classified correctly.

Table 4.14. Classification accuracies of each class for training data of wet impregnation base data set.

Experimental Data		**Predictions for Training**			
Conversion	Number of data	0-50	50-75	75-100	Classification Accuracy (%)
0-50	741	**668**	69	4	90.1
50-75	719	57	**610**	52	84.8
75-100	596	15	82	**499**	83.7

Table 4.15. Classification accuracies of each class for testing data of wet impregnation base data set.

Experimental Data		**Predictions for Testing**			
Conversion	Number of data	0-50	50-75	75-100	Classification Accuracy (%)
0-50	359	**323**	35	1	90.0
50-75	346	36	**288**	22	83.2
75-100	323	13	47	**263**	81.4

4.1.6. Analysis of H_2/CO Results Using Entire Data Set

The H_2/CO ratio base data including 2323 instances with 58 attributes were classified according to their H_2/CO ratios as 0-0.9 consisting of 1574 data, 0.9-2 consisting of 741 data and 2-3.3 consisting of 8 data. These classes were created depending on the objective of DRM reaction. The H_2/CO ratio is important for further use and it should be equal to or less than 1 to use in Fischer-Tropsch synthesis and in the production of formaldehyde, polycarbonates or methanol. The main advantage of DRM to steam reforming of methane is that DRM produces high purity syngas containing little CO_2 with $H_2/CO \leq 1$ so there is no need to remove CO_2 [1]. Therefore higher H_2/CO ratio is not preferred for DRM. 1549 instances were used as training and the remaining 774 instances were used as testing set. The optimal decision tree was found by starting with a large tree and then 10 levels of pruning were applied to the fully grown tree until the minimum test error rate was found. The training and test error rates for various tree sizes having the splitmin value 150 were shown in Figure 4.11. The tree with the minimum test error percentages was found with 27 nodes, corresponding to prune level 1, training and test errors of 11.6% and 14.1%, respectively. The optimal decision tree was shown in Figure 4.12.

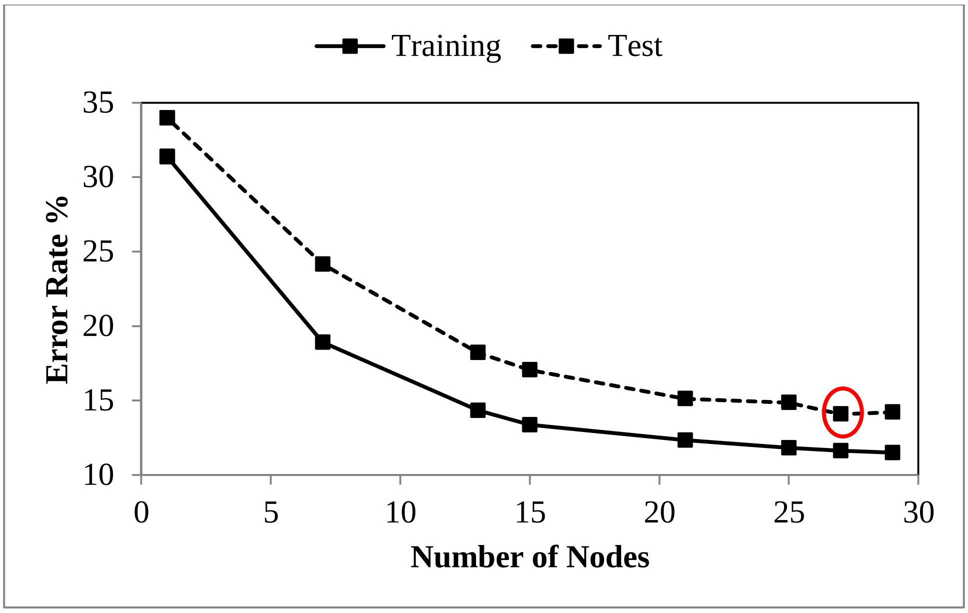

Figure 4.11. Training and test error rates of H_2/CO base data set.

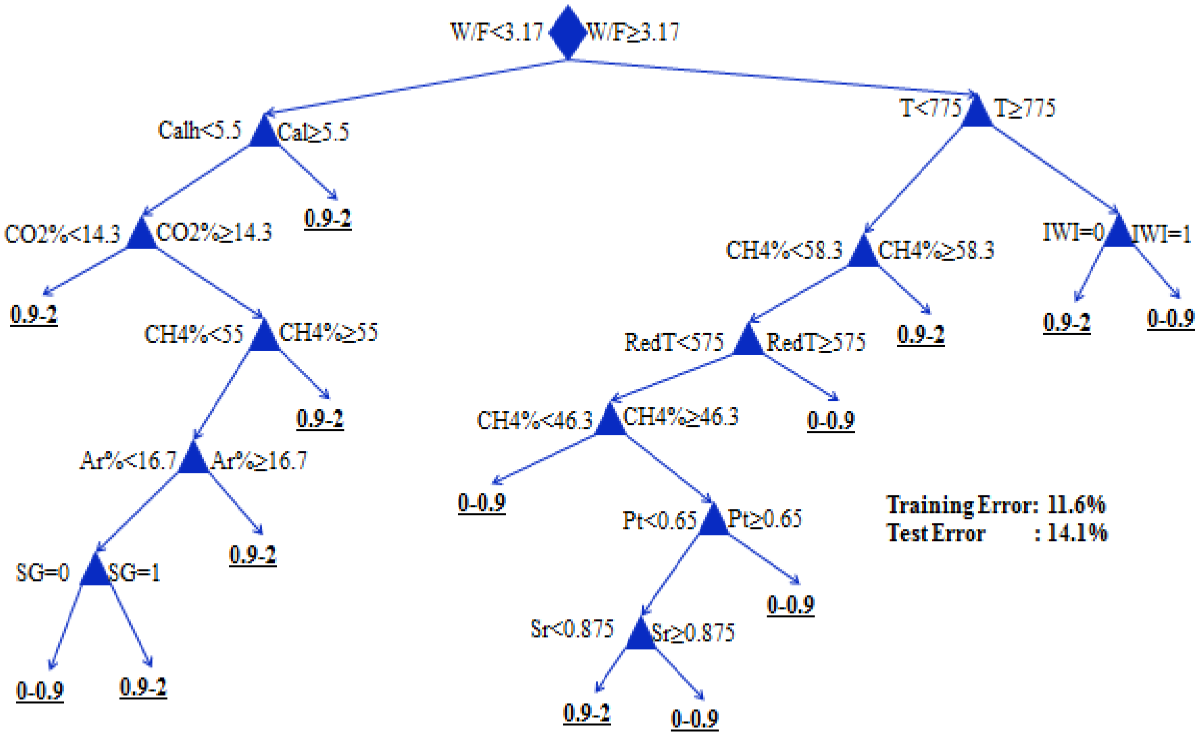

Figure 4.12. Optimal decision tree for H_2/CO base data.

Figure 4.12 reveals that the first division was done according to the value of W/F. W/F value that was lower than 3.17 resulted in 0.9-2 value except for the catalysts were not prepared by the sol-gel method at the leaf node. If W/F value was higher than 3.17, second division was done according to the reaction temperature. If the reaction temperature was higher than 775 °C, 0.9-2 interval was possible only if the catalysts were not prepared by incipient to wetness impregnation method. If the reaction temperature was lower than 775 °C, volumetric percentage of CH_4, reduction temperature and the amounts of Pt and Sr metals in catalysts became significant to reach 0.9-2 ratio value. The rules deduced from the tree were presented in Table 4.16.

Table 4.16. Rules for 0.9-2 H_2/CO values for H_2/CO base data.

W/F<3.17	Calh≥5.5						0.9-2
	Calh<5.5	CO2%≥14.3	CH4%≥55				0.9-2
			CH4%<55	Ar%≥16.7			0.9-2
				Ar%<16.7	SG		0.9-2
					IWI,WI,CI,CP,SI		0-0.9
		CO2%<14.3					0.9-2
W/F≥3.17	T≥775	IWI					0-0.9
		WI,CI,SI,CP,SG					0.9-2
	T<775	CH4%≥58.3					0.9-2
		CH4%<58.3	RedT≥575				0-0.9
			RedT<575	CH4%≥46.3	Pt≥0.65		0-0.9
					Pt<0.65	Sr≥0.875	0-0.9
						Sr<0.875	0.9-2
				CH4%<46.3			0-0.9

The confusion matrices belonging to optimum H_2/CO base tree for training and testing are presented in Table 4.17 and Table 4.18. Class imbalance problem can be seen in these matrices obviously. The other two classes dominated the class of 2-3.3 because 2-3.3 class had only 8 instances. And also this class was created for the chemical issues because purification process is needed for further use if H_2/CO ratio is higher than 2. 1369 data out of 1549 were classified correctly during training. 665 data out of 774 (85.9%) were classified correctly during testing.

Table 4.17. Classification accuracies of each class for training data of H_2/CO data set.

Experimental Data		**Predictions for Training**			
H_2/CO	Number of data	0-0.9	0.9-2	2-3.3	Classification Accuracy (%)
0-0.9	1063	**976**	87	0	91.8
0.9-2	482	89	**393**	0	81.5
2-3.3	4	3	1	**0**	0.0

Table 4.18. Classification accuracies of each class for testing data of H_2/CO data set.

Experimental Data		**Predictions for Testing**			
H_2/CO	Number of data	0-0.9	0.9-2	2-3.3	Classification Accuracy (%)
0-0.9	511	**464**	47	0	90.8
0.9-2	259	58	**201**	0	77.6
2-3.3	4	3	1	**0**	0.0

4.2. Artificial Neural Network Analyses for Input Significance and Prediction

4.2.1. Determining the Optimal Neural Network Topology

The optimum neural network topology was determined by using the value of testing RMSE and R^2 because they showed the ability of network to predict the unseen data. The RMSE of training was calculated by the error obtained between the experimental data points and the model predictions on the total data. The RMSE of testing was determined by 4-fold cross validation method as described in Chapter 3. Tangent sigmoid function was used as transfer function so the inputs and targets were normalized between -1 and +1. Trainlm and trainbr were used as training algorithms for training and testing, respectively.

Several network topologies were tested and compared with their RMSE values of training and testing. Only the results of one hidden layer networks are presented here because they produced almost the same results with two hidden layers. The training and testing errors of 21 networks with the increasing number of neurons in the first hidden layer are compared in Figure 4.13. The notation of a-b-c, the number in the x-axis, is used to label the neural networks. The meaning of this notation is that 63 input variables introduced through the increasing number of neurons ranged from 10 to 30 in the first hidden layer and 1 output variable (CH_4 conversion). Figure 4.13 shows that increasing the number of neurons in the hidden layer leads to the decrease in the training RMSE value as expected. However, testing RMSE value decreases first with the increasing network size and then starts to increase after reaching a minimum because of the overfitting. The network structure of 63-20-1 exhibits the minimum RMSE of testing (8.6622) with a considerably low RMSE of training (4.2278) so this structure was used in the remaining part of the study.

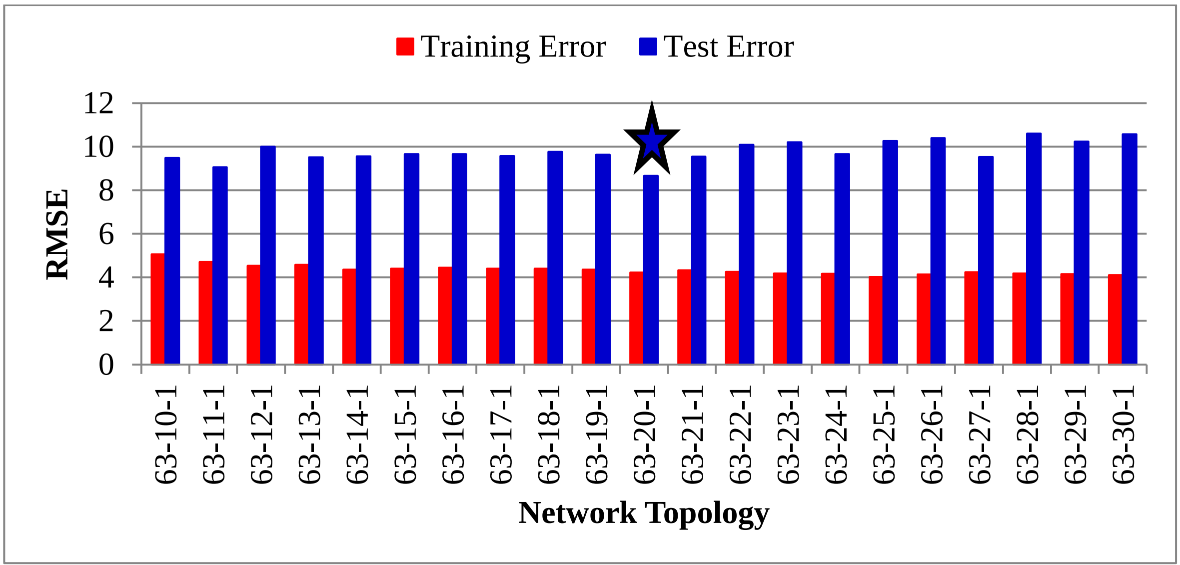

Figure 4.13. Training and testing errors of different neural network topologies.

The experimental versus predicted CH_4 conversion plots of the optimal network (63-20-1) for both training and testing are given in Figure 4.14, which indicates considerably successful fittings. The RMSE and corresponding R^2 values of training and testing are also quite satisfactory.

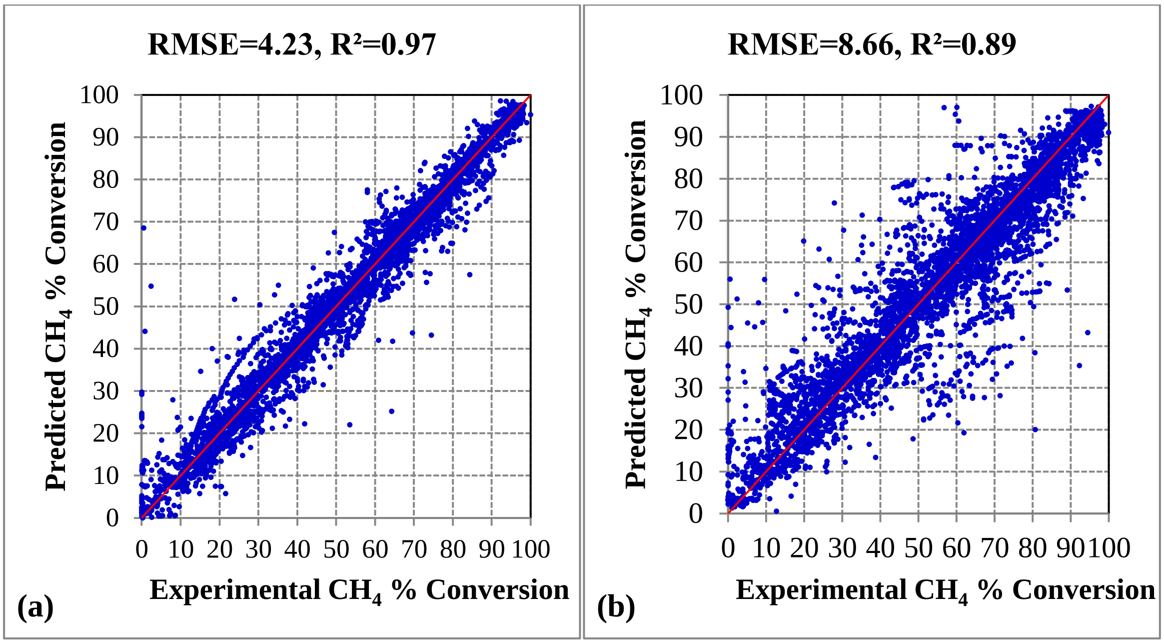

Figure 4.14. Experimental versus predicted CH_4 conversion for: (a) training, (b) testing data by the optimal neural network topology.

4.2.2. Analyzing the Input Significance

The relative significances of catalyst design and operational variables on CH_4 conversion were analyzed using the optimal neural network topology. The relative importance of input variables was calculated by the method of the change of root mean square error that is suitable for both categorical and continuous attributes. One of the input variables such as metal types removed from the data set and the network was trained with the remaining input variables. The RMSE value of the model calculated in the absence of these metals (8.59) was compared with the RMSE value calculated in the presence of all inputs (4.28). This procedure was repeated for all input variables. Finally, the difference between the RMSE values was used as the indicator of the relative input significance. The results are shown in Table 4.19. The catalyst design variables were found to have 45% relative significance while operational variables were found to have 55% relative significance. Operating variables were more important than the catalyst design variables, and also reaction temperature was found to be the most important factor affecting the CH_4 conversion level. This result was consistent with the nature of DRM reaction. After reaction temperature, weight percentages of metal types were found to be the second most significant variable with 20.6% relative significance and it was followed by support types with 18.1% relative significance. And also they were found to be the most important variables for effective catalyst design. Feed compositions especially the CH_4/CO_2 ratio and W/F were also important to reach desired conversion level.

Table 4.19. Relative significances of input variables for DRM reaction.

Input Variable	RMSE (found)	RMSE difference*	Relative Significance %	Group Significance %
Metal	8.59	4.31	20.6	Catalyst Design Variables 45
Support	8.07	3.79	18.1	
Reduction Conditions	4.92	0.64	3.1	
Calcination Conditions	4.72	0.44	2.1	
Catalyst Preparation Method	4.52	0.24	1.1	
Reaction Temperature	12.84	8.56	40.9	Operational Variables 55
Feed Compositions	5.61	1.32	6.3	
W/F	5.49	1.21	5.8	
TOS	4.68	0.40	1.9	

* the difference between RMSE without the variable or variables and RMSE of the original model (4.28)

It should be considered that the relative significances of the input variables were valid within the range of the total data set. Therefore the results should be used as suggestions to reach higher CH_4 conversion level, not an absolute rule.

4.2.3. Analyzing the Results of Unseen Papers

The prediction ability of optimal neural network structure was tested on experiments, which were not seen by the network during training. For this, the data from the same experiments were identified and collected in the same group first resulting 753 independent experiments in 101 papers. One experiment from 753 was removed and network was trained with the remaining experiments in order to predict the outputs of the removed experiment. This procedure was repeated for all experiments. For each experiment RMSE and R^2 values were calculated as the indicator of the prediction ability of the network. The predicted and the experimental values of CH_4 conversion corresponding experiments in the same paper were collected together to calculate the RMSE and R^2 value of that paper. As a result, the RMSE values of 590 out of 753 experiments and 65 out of 101 papers had lower than 15 and the R^2 values of 46 out of 101 papers had higher than 0.5. The performances of the optimal neural network in predicting the results of the papers are shown in Table 4.20, where successfully predicted results are written with red color. Plots of predicted versus experimental CH_4 conversions for the most successfully predicted six publications are shown in Figure 4.15. In addition to this, although some papers had RMSE values lower than 15, their R^2 values were lower than 0.5 and vice versa.

Table 4.20. Prediction errors of each publication for dry reforming of methane.

Article	**Number of Data**	**Number of Experiments**	**RMSE**	**Abs Error**	**R^2**
[10] (Xu *et al.*, 2012)	45	10	6.2	4.6	0.89
[28] (Al-Fatesh *et al.*, 2014)	165	25	4.7	3.5	0.95
[29] (Yang *et al.*, 2010)	9	9	11.7	8.1	0.00
[30] (Therdthianwong *et al.*, 2008)	12	10	20.4	17.1	0.16
[31] (Zanganeh *et al.*, 2013)	40	10	8.9	7.3	0.83
[32] (Li *et al.*, 2014)	5	1	9.6	8.8	0.73
[16] (Zhang *et al.*, 2008)	30	3	6.2	4.9	0.00
[33] (Pawelec *et al.*, 2007)	24	12	15.2	10.3	0.00
[34] (Rezaei *et al.*, 2008)	20	4	12.1	9.4	0.58
[35] (Meshkani and Rezaei, 2010)	16	4	23.3	18.3	0.00
[19] (Yasyerli *et al.*, 2011)	131	13	4.3	3.6	0.79
[36] (San-José-Alonso *et al.*, 2009)	10	5	13.3	10.2	0.00
[18] (Xu *et al.*, 2010)	16	4	9.4	6.5	0.86
[37] (Sengupta *et al.*, 2014)	24	4	12.6	10.8	0.00
[38] (Meili *et al.*, 2006)	28	7	8.2	5.6	0.40
[39] (Zhang *et al.*, 2005)	32	3	31.3	27.6	0.00
[40] (Lv *et al.*, 2012)	9	1	11.9	11.5	0.00
[41] (Pan *et al.*, 2008)	24	3	6.3	4.0	0.80
[42] (Nandini *et al.*, 2005)	251	21	9.5	8.2	0.53
[43] (Barroso-Quiroga and Castro-Luna, 2010)	46	6	21.9	18.6	0.00
[44] (Kambolis *et al.*, 2010)	38	8	11.2	8.0	0.00

Table 4.20. Prediction errors of each publication for dry reforming of methane (cont.).

[45] (Alipour *et al.*, 2014)	104	12	8.9	7.1	0.48
[13] (García *et al.*, 2009)	40	4	6.1	5.2	0.00
[46] (Meshkani *et al.*, 2014)	106	10	7.9	6.2	0.70
[47] (Alvar and Rezaei, 2009)	20	4	8.4	7.6	0.80
[48] (Hadian and Rezaei, 2013)	25	6	10.1	8.0	0.74
[49] (Chang *et al.*, 2006)	6	6	5.6	4.4	0.00
[50] (Moniri *et al.*, 2010)	36	5	15.0	12.6	0.65
[51] (Al-Fatesh and Fakeeha, 2012)	48	13	16.4	12.1	0.69
[52] (García-Diéguez *et al.*, 2010)	30	5	6.5	5.3	0.89
[53] (García-Diéguez *et al.*, 2010)	6	3	10.9	8.8	0.65
[14] (Xu *et al.*, 2012)	99	22	13.3	10.2	0.47
[54] (Yao *et al.*, 2013)	20	4	4.4	3.4	0.96
[55] (Zanganeh *et al.*, 2014)	9	3	28.8	18.7	0.00
[27] (Luisetto *et al.*, 2012)	53	6	3.7	3.3	0.91
[56] (Zhang *et al.*, 2008)	47	10	8.4	5.4	0.86
[57] (Özkara-Aydınoğlu and Aksoylu, 2011)	62	7	25.8	20.5	0.15
[58] (Rezaei *et al.*, 2009)	10	2	3.9	3.7	0.95
[59] (Al-Fatesh, 2013)	119	14	2.8	2.0	0.97
[60] (Wang *et al.*, 2013)	110	7	12.3	9.7	0.32
[61] (Liu *et al.*, 2010)	28	4	22.8	16.1	0.00
[62] (Tang *et al.*, 2014)	70	14	16.3	11.4	0.67
[63] (Naeem *et al.*, 2014)	15	6	13.8	9.2	0.74
[26] (Pompeo *et al.*, 2009)	30	6	12.4	11.1	0.65
[64] (Ranjbar and Rezaei, 2012)	123	13	4.5	3.8	0.88
[65] (Wang *et al.*, 2009)	9	1	33.7	29.0	0.00
[66] (Meshkani and Rezaei, 2011)	147	10	17.5	12.5	0.00
[67] (Hadian *et al.*, 2012)	111	10	4.8	4.0	0.79
[68] (Bellido and Assaf, 2009)	144	4	40.2	35.7	0.00
[69] (Pompeo *et al.*, 2005)	9	3	5.3	4.9	0.81
[70] (Fajardo *et al.*, 2005)	14	2	6.0	5.3	0.53
[2] (Alipour *et al.*, 2014)	128	14	5.0	3.9	0.85
[71] (Al-Fatesh *et al.*, 2011)	76	20	4.3	3.7	0.97
[72] (Juan-Juan *et al.*, 2006)	44	8	8.0	6.9	0.00
[73] (Halliche *et al.*, 2005)	12	1	27.0	26.2	0.00
[74] (Fakeeha *et al.*, 2013)	24	8	7.7	6.8	0.91
[75] (Vafaeian *et al.*, 2013)	24	4	16.2	14.0	0.34
[76] (Takanabe *et al.*, 2005)	85	7	15.4	11.1	0.00

Table 4.20. Prediction errors of each publication for dry reforming of methane (cont.).

[20] (Serrano-Lotina and Daza, 2014)	20	3	15.4	8.7	0.60
[77] (Zanganeh *et al*., 2013)	24	2	16.9	14.1	0.00
[78] (Abdollahifar *et al*., 2014)	6	1	7.5	6.1	0.93
[79] (Gonzaléz *et al*., 2013)	174	9	14.2	10.9	0.00
[80] (Khajenoori *et al*., 2014)	81	12	5.3	4.2	0.87
[81] (Xu *et al*., 2009)	140	5	10.1	9.0	0.81
[82] (Qian *et al*., 2014)	54	6	3.8	3.0	0.88
[83] (Luengnaruemitchai and Kaengsilalai, 2008)	48	3	19.3	16.0	0.00
[84] (Jóźwiak *et al*., 2005)	7	7	7.7	6.5	0.00
[85] (Taufiq-Yap *et al*., 2013)	162	12	6.0	3.0	0.90
[86] (Wu *et al*., 2014)	70	7	14.7	8.2	0.83
[87] (Ocsachoque *et al*., 2011)	9	9	7.5	6.2	0.41
[88] (Bellido *et al*., 2009)	144	4	36.2	32.2	0.00
[89] (Nagaraja *et al*., 2011)	25	5	8.2	6.4	0.85
[90] (Razaei *et al*., 2008)	75	6	7.6	6.7	0.87
[91] (Al-Fatish *et al*., 2009)	40	11	26.6	16.9	0.00
[92] (Hou *et al*., 2006)	36	20	28.4	21.3	0.00
[93] (Habibi *et al*., 2014)	119	8	5.2	4.5	0.81
[94] (Newnham *et al*., 2012)	20	1	21.1	19.0	0.00
[95] (Damyanova *et al*., 2011)	18	2	13.8	10.2	0.37
[96] (García-Diéguez *et al*., 2010)	8	4	7.7	6.6	0.51
[6] (Tankov *et al*., 2014)	100	10	7.6	6.1	0.36
[97] (Mirzaei *et al*., 2014)	91	12	18.6	16.5	0.12
[98] (Nematollahi *et al*., 2014)	16	3	7.4	6.0	0.90
[99] (Fakeeha *et al*., 2014)	28	14	4.1	3.3	0.98
[100] (Lee *et al*., 2014)	20	8	30.0	21.7	0.00
[101] (Shi and Zhang, 2012)	30	6	30.4	24.9	0.00
[102] (Ballarini *et al*., 2012)	12	6	34.0	32.7	0.00
[103] (Sarusi *et al*., 2011)	70	10	2.3	1.7	0.00
[104] (Shang *et al*., 2011)	52	15	9.3	5.7	0.00
[105] (Nematollahi *et al*., 2011)	25	5	8.6	7.3	0.84
[106] (José-Alonso *et al*., 2011)	5	5	22.0	17.8	0.00
[11] (Özkara-Aydınoğlu and Aksoylu, 2010)	78	8	28.7	24.7	0.00
[107] (Reddy *et al*., 2010)	160	5	37.2	35.6	0.00
[108] (Damyanova *et al*., 2009)	96	6	7.1	4.8	0.00
[15] (Özkara-Aydınoğlu *et al*., 2009)	84	12	21.0	16.3	0.00
[109] (Xiancai *et al*., 2008)	12	4	9.1	6.2	0.00

Table 4.20. Prediction errors of each publication for dry reforming of methane (cont.).

[110] (Rui *et al*., 2007)	3	3	20.8	19.8	0.00
[111] (Rezaei *et al*., 2006)	165	20	5.8	4.3	0.91
[112] (Yang and Papp, 2006)	18	2	21.0	17.0	0.24
[113] (Ballarini *et al*., 2005)	40	7	17.4	12.6	0.24
[114] (Bouarab *et al*., 2005)	24	4	22.2	19.6	0.00
[17] (Takanabe *et al*., 2005)	94	10	19.5	16.1	0.23

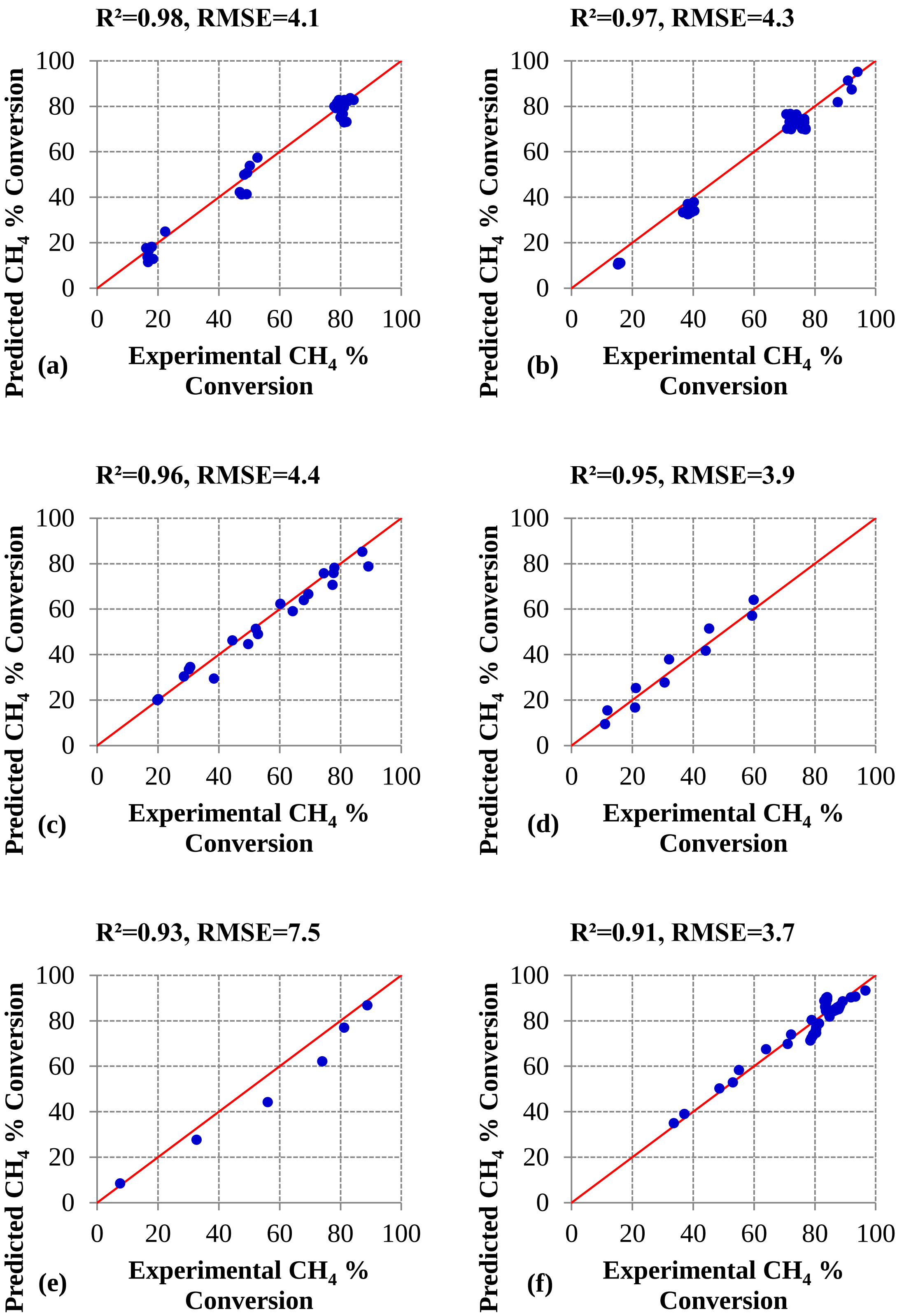

Figure 4.15. Experimental vs. predicted CH_4 conversion for: (a) Fakeeha *et al*. [99], (b) Al-Fatesh *et al*. [71], (c) Yao *et al*. [54], (d) Rezaei *et al*. [58], (e) Abdollahifar *et al*. [78], (f) Luisetto *et al*. [27].

4.2.4. Analyzing the Effects of Catalyst Variables

The effect of the weight percentage of Ni was studied by Xu *et al*. (2012). This paper was one of those used to test the prediction of variable effects. Ni was used with the weight percentages of 3, 5, 7, 10 and 15% over ordered mesoporous alumina having large specific surface area, big pore volume, uniform pore size and high thermal stability. The conversion values were observed in different reaction temperatures ranged from 600 to 800 with given reaction conditions (CH_4/CO_2=1, W/F=4 mgmin/ml (=15000ml/hg_{cat}) and TOS= 60 min). The conversion of CH_4 increased until reached to 5 wt.%Ni content for all the temperature ranges. Increasing the Ni content up to 15 wt.% resulted in slight improvement in the CH_4 conversion. 5 wt.%Ni showed the better catalytic performance for DRM reaction. The RMSE and corresponding R^2 values of the experiments were 8.4-0.89, 4.1-0.96, 1.7-0.99, 2.5-0.98, 6.3-0.88, respectively. The experimental results in Figure 4.16 are quite close to the neural network predictions. [10].

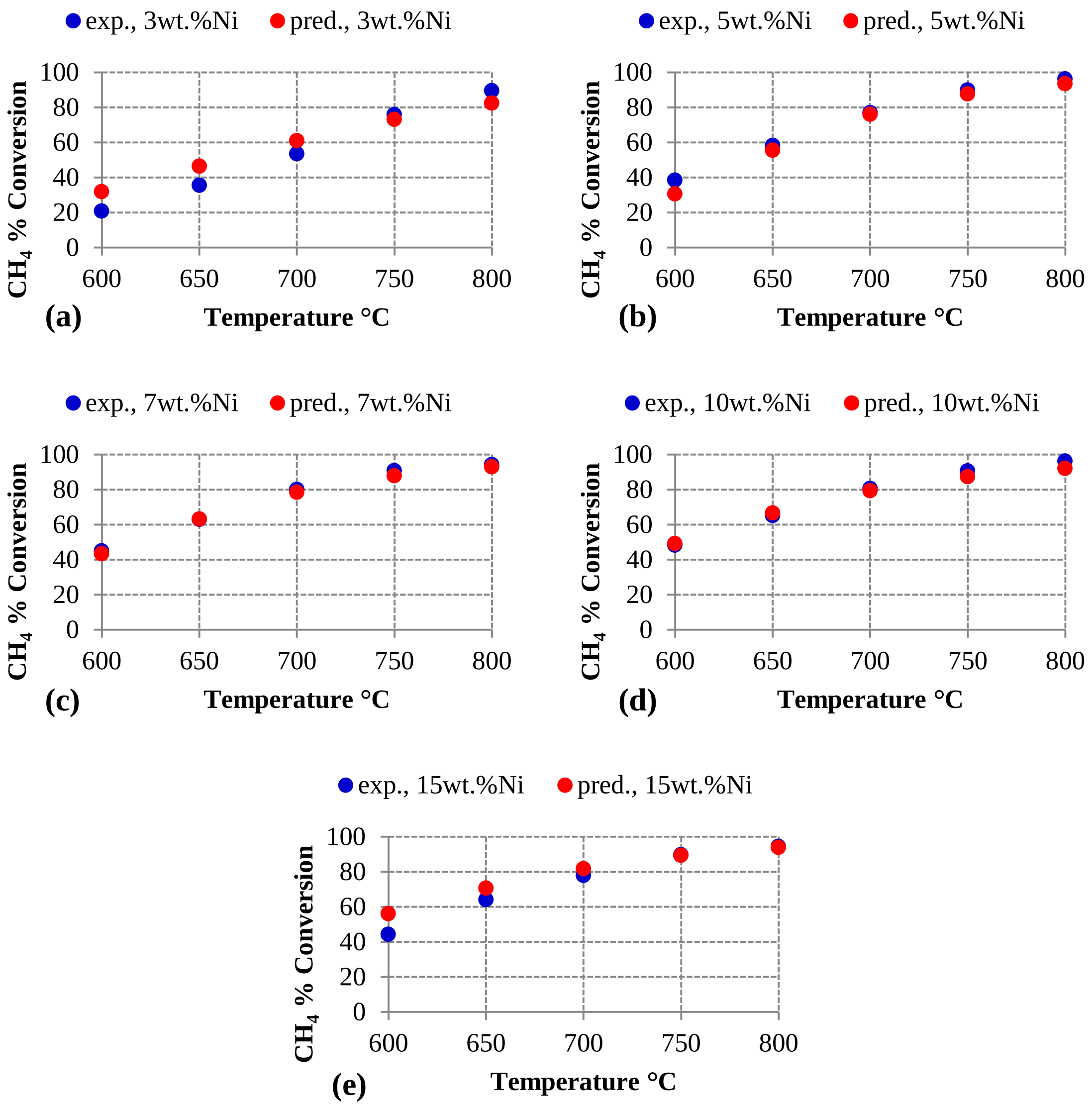

Figure 4.16. The effect of Ni loading on CH_4 conversion on meso-Al_2O_3: (a) 3 wt.%, (b) 5 wt.%, (c) 7 wt.%, (d) 10 wt.% and (e) 15 wt.% [10].

The effect of calcination temperature on CH_4 conversion was investigated for TiO_2-SiO_2 supported Ni catalysts through the work of Zhang *et al*. (2008). Reaction conditions were T=700 °C, CH_4/CO_2=1, W/F=1.67 mgmin/ml (=36000ml/hg_{cat}). They reported that the catalyst calcined at 700 °C showed better activity and stability than the catalyst calcined at 550 °C. The RMSE values of the experiments were 0.8 for the catalyst calcined at 550 °C and 8.7 for the catalyst calcined at 700 °C. If the calcination temperature was raised to 850 °C a large amount of coke deposited on the catalyst and led to plugging of the reactor in 2 h of the reaction. The experimental results in Figure 4.17 are quite close to the neural network predictions [16].

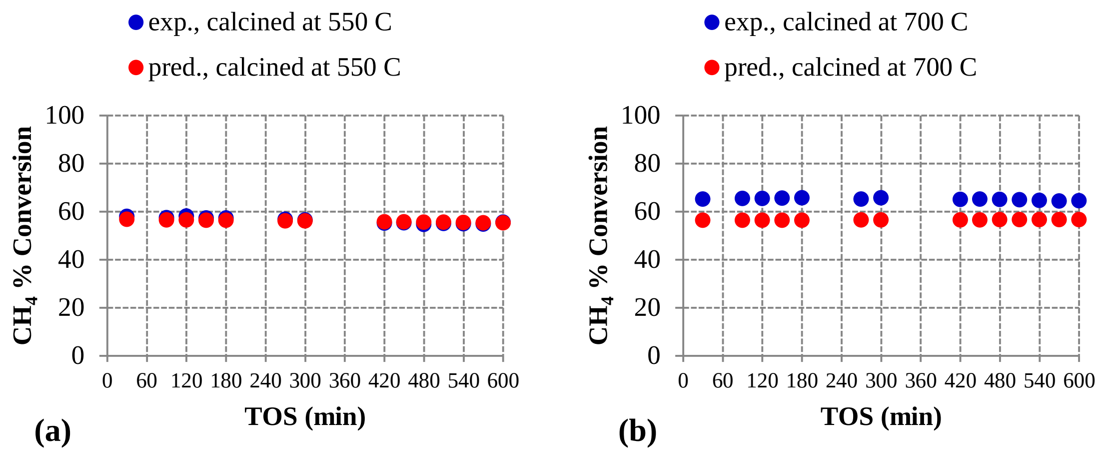

Figure 4.17. Effect of calcination temperature on CH_4 conversion for Ni/TiO_2-SiO_2 catalyst: (a) calcined at 550 °C and (b) calcined at 700 °C [16].

In the study of García-Diéguez *et al*. (2010), monometallic (Ni and Pt) and bimetallic (PtNi) catalysts supported on γ-Al_2O_3 were used to comprehend the effect of second metal addition on CH_4 conversion. An important difference between CH_4 conversion values for any of the PtNi catalysts were not observed in the temperature range of 400-600 °C. The conversion values rose between 600-700 °C. The bimetallic PtNi catalyst had a good performance in the DRM reaction at 700 °C in terms of stability and activity because addition of Pt prevented coke deposition and improved the stability and activity of Ni-based catalysts for DRM reaction. The experimental results in Figure 4.18 are quite close to the neural network predictions (the RMSE and corresponding R^2 values of the experiments were 3.5-0.97, 6.1-0.90, 3.9-0.97, 7.5-0.88, respectively) [52].

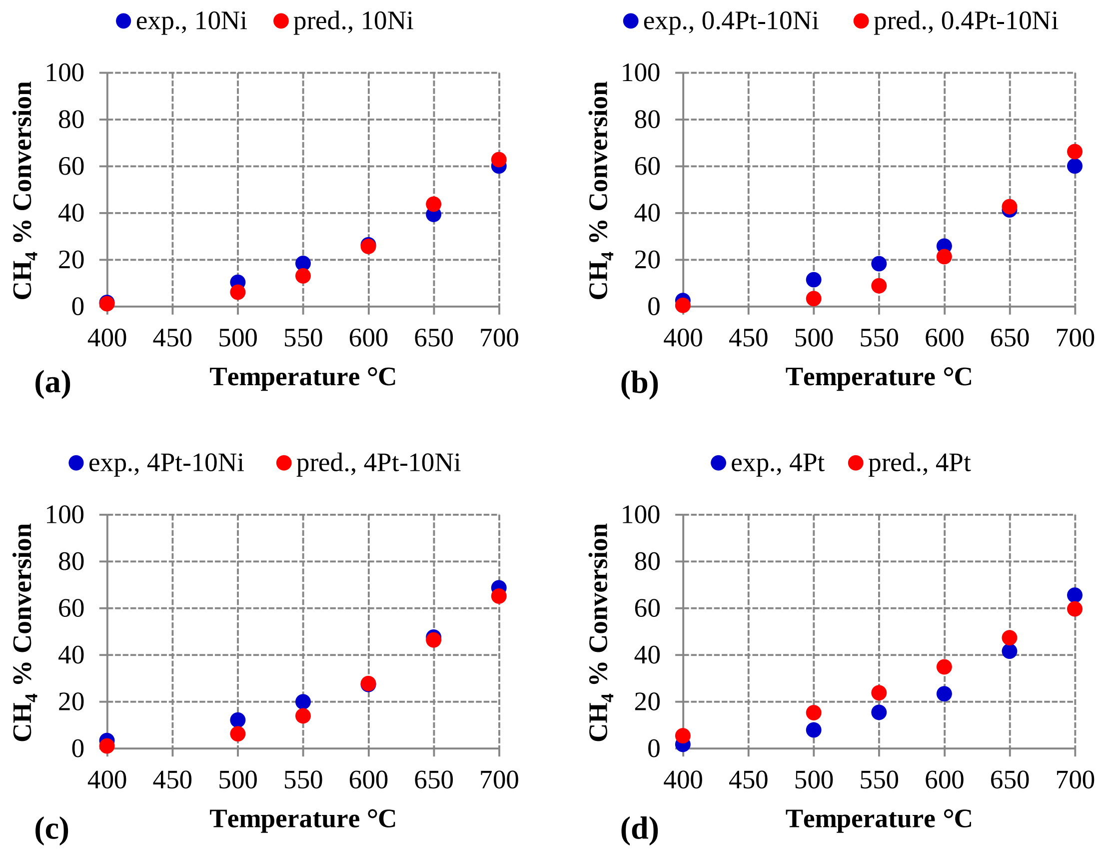

Figure 4.18. Effect of base metal and the amount of second metal addition on CH_4 conversion: (a) 10 wt.%Ni, (b) 0.4 wt.%Pt-10 wt.%Ni, (c) 4 wt.%Pt-10 wt.%Ni and (d) 4 wt.%Pt [52].

Finally, the effect of Ce/Zr ratio in the support was investigated by Xu *et al.* (2012). Ni was used as base metal with a fixed weight percentage (7%). Different Ce/Zr ratios were used and the change of CH_4 conversions was observed with the temperature ranged from 600-800 °C. The catalyst supported on 50/50 Ce/Zr ratio had higher catalytic activity and better catalytic stability because the activation of CO_2 was promoted by the redox property of mesoporous CeZr support. The experimental results in Figure 4.19 are quite close to the neural network predictions (the RMSE values of the experiments were 12.8, 11.2, 12.4, 6.7, 6.3, 5.9, respectively) [14].

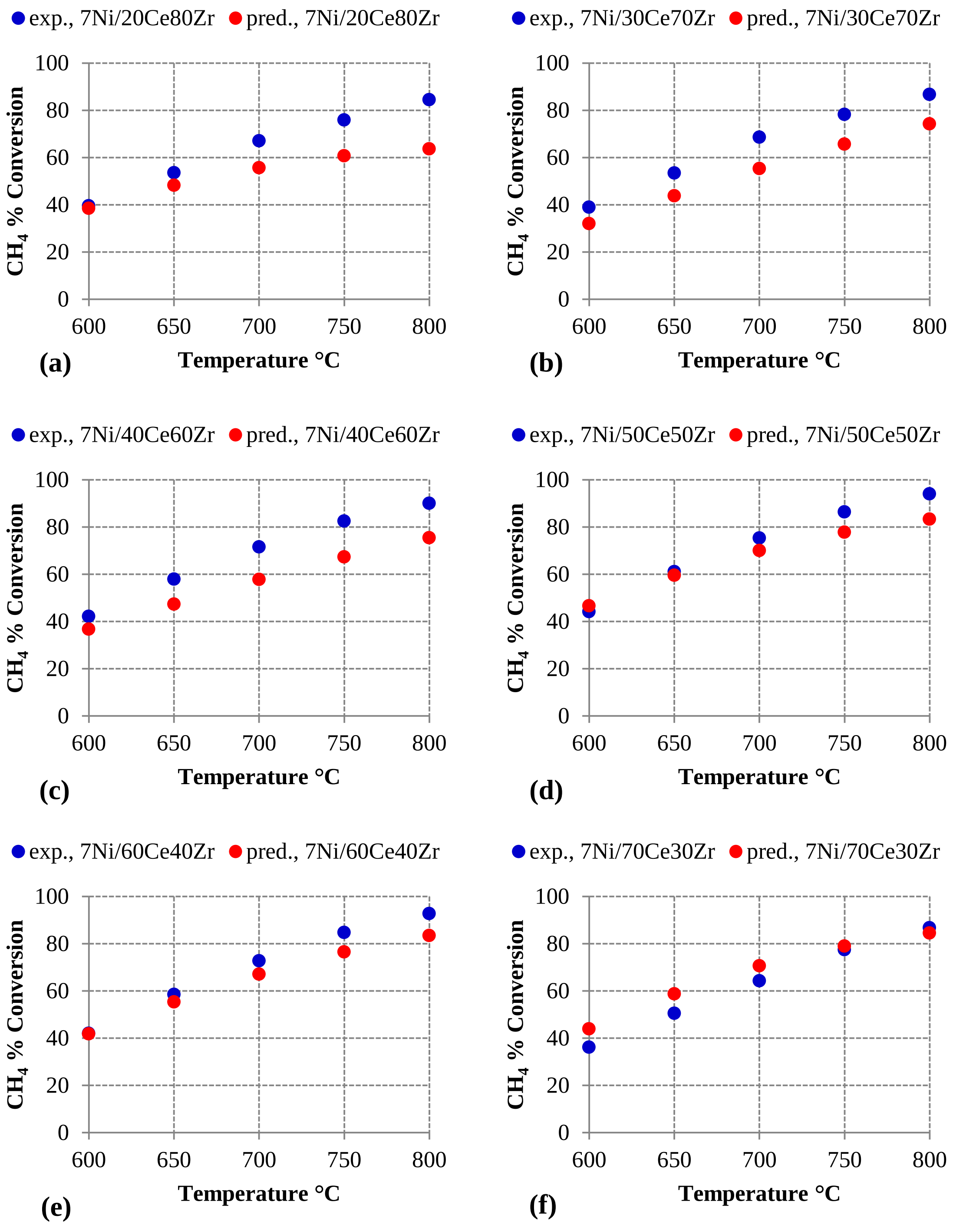

Figure 4.19. Effect of Ce/Zr ratio in the support on CH_4 conversion [14].

5. CONCLUSIONS AND RECOMMENDATIONS

5.1. Conclusions

The aim of this thesis was to extract knowledge from experimental data using data mining techniques. The experimental data for DRM reaction were collected from the papers published between the years of 2005-2014. The final data set consisted of 101 papers including 5521 experimental data with 63 attributes and 3 output variables (CH_4 conversion, CO_2 conversion and H_2/CO ratio; CO_2 conversion was not used in analyses). Two different data mining techniques that are decision trees and artificial neural networks were applied to the final data set to extract valuable knowledge for DRM reaction.

Total data set, Ni base, Co base, Pt base and wet impregnation base data sets were analyzed by decision trees classifying the CH_4 conversion values. Apart from these trees, H_2/CO results were also used as the output values for decision tree classification of total data. The optimal decision trees were found by using different splitmin and prune values. For each splitmin values, 10 levels of pruning were applied to the large tree until the minimum test error rate was found. The optimal tree structure for total data set was found with the splitmin value of 150 and pruning level of 5. This tree had 39 nodes with training and test error of 21.1% and 21.5%, respectively. The tree of Ni base data having splitmin value of 125 and pruning level of 6 had 43 nodes with training and test error of 16.7% and 19.0%, respectively. The tree of Co base data having splitmin value of 25 was found with 21 nodes corresponding to the prune level of 3, training and test errors of 10.2% and 10.9%, respectively. The splitmin value, number of nodes with corresponding prune level, training and test errors for Pt base tree were 25, 27-2, 9.3% and 12.6%, respectively. The splitmin value, number of nodes with corresponding prune level, training and test errors for wet impregnation base tree were 100, 39-3, 13.6% and 15.1%, respectively. First division for these trees was done by reaction temperature except for Co base tree (first division was done by calcination temperature for this case). The division by reaction temperature was consistent with the results of input significance and endothermicity of the reaction. The optimal tree structure for the data set of H_2/CO outputs was found with the splitmin value of 150 and pruning level of 1. This tree had 27 nodes with training and test error of 11.6% and 14.1%, respectively. The confusion matrices were formed in order to comprehend the distribution of correctly and incorrectly predicted data among the classes. The higher and lower conversion levels seem to be placed to the correct classes more accurately compared to the middle level.

In the ANN analysis, trainlm and trainbr were used as training algorithms for training and testing, respectively. Tangent sigmoid function was used as activation function. Various number of neurons in one hidden layer were tried to find optimal neural network structure. The prediction ability of test data is more valuable than the prediction ability of training data so the optimal neural network topology was selected using the RMSE value of testing that was calculated by 4-fold cross validation technique. 20 neurons in one hidden layer produced the best result with the RMSE value of 8.66 in testing.

The input significance results showed that the catalyst preparation and operating variables were found to be effective on the activity of catalysts. The relative significances of the preparation variables from the most significant to the lowest one were found as metal types and amount, support type, reduction conditions, calcination conditions and catalyst preparation methods. Reaction temperature was the most important variable (with the relative significance of 40.9%) followed by feed compositions, W/F and TOS. It should also be stated that operational variables (55%) had higher group significance than the catalyst design variables (45%) within the range of total data set.

The prediction abilities of the optimal model were firstly tested on each experiment. 590 out of 753 experiments (78.4%) were predicted with RMSE values lower than 15. Finally, the performance of the model was tested on each article. The results of 46 out of 101 papers (45.5%) were predicted with R^2 values higher than 0.5 and the RMSE values of 65 out of 101 papers (64.4%) had lower than 15.

As a result, decision tree, as a widely used classification technique because of its simplicity and interpretability, could be also converted into a set of rules and these rules easily provide knowledge extraction in this work. On the other hand, the results of neural network were not easily interpreted because of the complexity of its structure. Despite all its disadvantages however, artificial neural networks seemed to have some prediction ability for DRM reactions, hence it could be used to extract knowledge from published experimental data and used it to plan the future experiments.

5.2. Recommendations

The following recommendations can be made based on the results obtained from this thesis to improve the analyses:

- The data set can be extended collecting data from the papers published earlier than 2005 and later than 2014.
- There may be additional attributes that were not reported by publishers.
- In classifying with decision tree analysis, class distribution was imbalanced. This can produce some problems for existing algorithm.
- Postprocessing techniques can be applied to the decision tree results in order to integrate only valid results into information.
- Parameter optimization for ANN can be done using other methods except for 4-fold cross validation technique. Although leave one out cross validation technique is computationally expensive and takes more time; however, the optimized parameters using this technique may produce better results in ANN analysis.
- Instead of applying neural network to the data set directly, various preprocessing techniques can be applied to the total data set. Clustering analysis of the total data set is highly recommended to describe data set firstly. And the results obtained from the clustering analysis can be used as inputs for other algorithms.
- Neural networks can be applied to more than one output. Therefore the conversion of CH_4 together with CO_2 can be used as outputs in a model when the reaction mechanism is taken into account.
- For DRM reaction, results of generally conducted experiments are shown in the figures as methane conversion versus time on stream, reaction temperature, gas hourly space velocity and CH_4/CO_2 ratio. Therefore database can be separated in terms of these four types of experiments and each type of experiments can be modeled separately. For example, one model can be constructed using the data of methane conversion with changing reaction temperature.

- Other data mining techniques such as support vector machine and decision tree regression can be used for modeling.

REFERENCES

1. Pakhare, D. and J. Spivey, "A Review of Dry (CO_2) Reforming of Methane over Noble Metal Catalysts", *Chemical Society Reviews*, Vol. 43, No. 22, pp. 7813-7837, 2014.

2. Alipour, Z., M. Rezaei, and F. Meshkani, "Effect of Alkaline Earth Promoters (MgO, CaO, and BaO) on the Activity and Coke Formation of Ni Catalysts Supported on Nanocrystalline Al_2O_3 in Dry Reforming of Methane", *Journal of Industrial and Engineering Chemistry*, Vol. 20, No. 5, pp. 2858-2863, 2014.

3. Cai, W.-J., L.-P. Qian, B. Yue, and H.-Y. He, "Rh Doping Effect on Coking Resistance of Ni/SBA-15 Catalysts in Dry Reforming of Methane", *Chinese Chemical Letters*, Vol. 25, No. 11, pp. 1411-1415, 2014.

4. Lovell, E., Y. Jiang, J. Scott, F. Wang, Y. Suhardja, M. Chen, J. Huang, and R. Amal, "CO_2 Reforming of Methane over MCM-41-Supported Nickel Catalysts: Altering Support Acidity by One-Pot Synthesis at Room Temperature", *Applied Catalysis A: General*, Vol. 473, No. 1, pp. 51-58, 2014.

5. Budiman, A., S.-H. Song, T.-S. Chang, C.-H. Shin, and M.-J. Choi, "Dry Reforming of Methane over Cobalt Catalysts: A Literature Review of Catalyst Development", *Catalysis Surveys from Asia*, Vol. 16, No. 4, pp. 183-197, 2012.

6. Tankov, I., K. Arishtirova, J. M. C. Bueno, and S. Damyanova, "Surface and Structural Features of Pt/PrO_2–Al_2O_3 Catalysts for Dry Methane Reforming", *Applied Catalysis A: General*, Vol. 474, No. 1, pp. 135-148, 2014.

7. Tan, P. N., M. Steinbach, and V. Kumar, *Introduction to Data Mining*, Pearson Addison Wesley, Boston, pp. 1-256, 2006.

8. Larose, D. T., *Discovering Knowledge in Data: An Introduction to Data Mining*, Wiley-Interscience, Hoboken, N.J., pp. 107-137, 2005.

9. Tuffery, S., *Data Mining and Statistics for Decision Making*, Wiley, Hoboken, N.J., pp. 217-320, 2011.

10. Xu, L., H. Zhao, H. Song, and L. Chou, "Ordered Mesoporous Alumina Supported Nickel Based Catalysts for Carbon Dioxide Reforming of Methane", *International Journal of Hydrogen Energy*, Vol. 37, No. 9, pp. 7497-7511, 2012.

11. Özkara-Aydınoğlu, Ş. and A. E. Aksoylu, "Carbon Dioxide Reforming of Methane over Co-X/ZrO_2 Catalysts (X=La, Ce, Mn, Mg, K)", *Catalysis Communications*, Vol. 11, No. 15, pp. 1165-1170, 2010.

12. Ross, J. R. H., *Heterogeneous Catalysis: Fundamentals and Applications*, Elsevier, Amsterdam, pp. 83-84, 2012.

13. García, V., J. J. Fernández, W. Ruíz, F. Mondragón, and A. Moreno, "Effect of MgO Addition on the Basicity of Ni/ZrO_2 and on Its Catalytic Activity in Carbon Dioxide Reforming of Methane", *Catalysis Communications*, Vol. 11, No. 4, pp. 240-246, 2009.

14. Xu, L., H. Song, and L. Chou, "Mesoporous Nanocrystalline Ceria–Zirconia Solid Solutions Supported Nickel Based Catalysts for CO_2 Reforming of CH_4", *International Journal of Hydrogen Energy*, Vol. 37, No. 23, pp. 18001-18020, 2012.

15. Özkara-Aydınoğlu, Ş., E. Özensoy, and A. E. Aksoylu, "The Effect of Impregnation Strategy on Methane Dry Reforming Activity of Ce Promoted Pt/ZrO_2", *International Journal of Hydrogen Energy*, Vol. 34, No. 24, pp. 9711-9722, 2009.

16. Zhang, S., J. Wang, and X. Wang, "Effect of Calcination Temperature on Structure and Performance of Ni/TiO_2-SiO_2 Catalyst for CO_2 Reforming of Methane", *Journal of Natural Gas Chemistry*, Vol. 17, No. 2, pp. 179-183, 2008.

17. Takanabe, K., K. Nagaoka, K. Nariai, and K.-i. Aika, "Influence of Reduction Temperature on the Catalytic Behavior of Co/TiO_2 Catalysts for CH_4/CO_2 Reforming and Its Relation with Titania Bulk Crystal Structure", *Journal of Catalysis*, Vol. 230, No. 1, pp. 75-85, 2005.

18. Xu, J., W. Zhou, Z. Li, J. Wang, and J. Ma, "Biogas Reforming for Hydrogen Production over a Ni–Co Bimetallic Catalyst: Effect of Operating Conditions", *International Journal of Hydrogen Energy*, Vol. 35, No. 23, pp. 13013-13020, 2010.

19. Yasyerli, S., S. Filizgok, H. Arbag, N. Yasyerli, and G. Dogu, "Ru Incorporated Ni–MCM-41 Mesoporous Catalysts for Dry Reforming of Methane: Effects of Mg Addition, Feed Composition and Temperature", *International Journal of Hydrogen Energy*, Vol. 36, No. 8, pp. 4863-4874, 2011.

20. Serrano-Lotina, A. and L. Daza, "Influence of the Operating Parameters over Dry Reforming of Methane to Syngas", *International Journal of Hydrogen Energy*, Vol. 39, No. 8, pp. 4089-4094, 2014.

21. Alpaydın, E., *Introduction to Machine Learning*, Vol. 2, The MIT Press, Cambridge, pp. 8-292, 2010.

22. Kantardzic, M., *Data Mining: Concepts, Models, Methods, and Algorithms*, Wiley-Interscience, Hoboken, N.J., pp. 195-213, 2003.

23. Beale, M. H., M. T. Hagan, and H. B. Demuth, "Neural Network Toolbox™ User's Guide", 2015, https://www.mathworks.com/help/pdf_doc/nnet/nnet_ug.pdf, [Accessed June 2015].

24. Günay, M. E., *Knowledge Extraction from Experimental and Computational Data for Selective CO Oxidation and Water Gas Shift Reaction Using Data Mining Techniques*, Ph.D. Thesis, Boğaziçi University, 2012.

25. Odabaşı, Ç., M. E. Günay, and R. Yıldırım, "Knowledge Extraction for Water Gas Shift Reaction over Noble Metal Catalysts from Publications in the Literature between 2002 and 2012", *International Journal of Hydrogen Energy*, Vol. 39, No. 11, pp. 5733-5746, 2014.

26. Pompeo, F., D. Gazzoli, and N. N. Nichio, "Stability Improvements of Ni/α-Al_2O_3 Catalysts to Obtain Hydrogen from Methane Reforming", *International Journal of Hydrogen Energy*, Vol. 34, No. 5, pp. 2260-2268, 2009.

27. Luisetto, I., S. Tuti, and E. Di Bartolomeo, "Co and Ni Supported on CeO_2 as Selective Bimetallic Catalyst for Dry Reforming of Methane", *International Journal of Hydrogen Energy*, Vol. 37, No. 21, pp. 15992-15999, 2012.

28. Al-Fatesh, A. S., M. A. Naeem, A. H. Fakeeha, and A. E. Abasaeed, "Role of La_2O_3 as Promoter and Support in Ni/γ-Al_2O_3 Catalysts for Dry Reforming of Methane", *Chinese Journal of Chemical Engineering*, Vol. 22, No. 1, pp. 28-37, 2014.

29. Yang, R., C. Xing, C. Lv, L. Shi, and N. Tsubaki, "Promotional Effect of La_2O_3 and CeO_2 on Ni/γ-Al_2O_3 Catalysts for CO_2 Reforming of CH_4", *Applied Catalysis A: General*, Vol. 385, No. 1–2, pp. 92-100, 2010.

30. Therdthianwong, S., C. Siangchin, and A. Therdthianwong, "Improvement of Coke Resistance of Ni/Al_2O_3 Catalyst in CH_4/CO_2 Reforming by ZrO_2 Addition", *Fuel Processing Technology*, Vol. 89, No. 2, pp. 160-168, 2008.

31. Zanganeh, R., M. Rezaei, and A. Zamaniyan, "Dry Reforming of Methane to Synthesis Gas on NiO–MgO nanocrystalline Solid Solution Catalysts", *International Journal of Hydrogen Energy*, Vol. 38, No. 7, pp. 3012-3018, 2013.

32. Li, J. F., C. Xia, C. T. Au, and B. S. Liu, "Y_2O_3-Promoted NiO/SBA-15 Catalysts Highly Active for CO_2/CH_4 Reforming", *International Journal of Hydrogen Energy*, Vol. 39, No. 21, pp. 10927-10940, 2014.

33. Pawelec, B., S. Damyanova, K. Arishtirova, J. L. G. Fierro, and L. Petrov, "Structural and Surface Features of Ptni Catalysts for Reforming of Methane with CO_2", *Applied Catalysis A: General*, Vol. 323, No. 1, pp. 188-201, 2007.

34. Rezaei, M., S. M. Alavi, S. Sahebdelfar, P. Bai, X. Liu, and Z.-F. Yan, "CO_2 Reforming of CH_4 over Nanocrystalline Zirconia-Supported Nickel Catalysts", *Applied Catalysis B: Environmental*, Vol. 77, No. 3–4, pp. 346-354, 2008.

35. Meshkani, F. and M. Rezaei, "Nanocrystalline MgO Supported Nickel-Based Bimetallic Catalysts for Carbon Dioxide Reforming of Methane", *International Journal of Hydrogen Energy*, Vol. 35, No. 19, pp. 10295-10301, 2010.

36. San-José-Alonso, D., J. Juan-Juan, M. J. Illán-Gómez, and M. C. Román-Martínez, "Ni, Co and Bimetallic Ni–Co Catalysts for the Dry Reforming of Methane", *Applied Catalysis A: General*, Vol. 371, No. 1–2, pp. 54-59, 2009.

37. Sengupta, S., K. Ray, and G. Deo, "Effects of Modifying Ni/Al_2O_3 Catalyst with Cobalt on the Reforming of CH_4 with CO_2 and Cracking of CH_4 Reactions", *International Journal of Hydrogen Energy*, Vol. 39, No. 22, pp. 11462-11472, 2014.

38. Zhang, M., S. Ji, L. Hu, F. Yin, C. Li, and H. Liu, "Structural Characterization of Highly Stable Ni/SBA-15 Catalyst and Its Catalytic Performance for Methane Reforming with CO_2", *Chinese Journal of Catalysis*, Vol. 27, No. 9, pp. 777-781, 2006.

39. Zhang, W. D., B. S. Liu, C. Zhu, and Y. L. Tian, "Preparation of La_2NiO_4/ZSM-5 Catalyst and Catalytic Performance in CO_2/CH_4 Reforming to Syngas", *Applied Catalysis A: General*, Vol. 292, No. 1, pp. 138-143, 2005.

40. Lv, X., J.-F. Chen, Y. Tan, and Y. Zhang, "A Highly Dispersed Nickel Supported Catalyst for Dry Reforming of Methane", *Catalysis Communications*, Vol. 20, No. 1, pp. 6-11, 2012.

41. Pan, Y.-X., C.-J. Liu, and P. Shi, "Preparation and Characterization of Coke Resistant Ni/SiO_2 Catalyst for Carbon Dioxide Reforming of Methane", *Journal of Power Sources*, Vol. 176, No. 1, pp. 46-53, 2008.

42. Nandini, A., K. K. Pant, and S. C. Dhingra, "K-, CeO_2-, and Mn-Promoted Ni/Al_2O_3 Catalysts for Stable CO_2 Reforming of Methane", *Applied Catalysis A: General*, Vol. 290, No. 1–2, pp. 166-174, 2005.

43. Barroso-Quiroga, M. M. and A. E. Castro-Luna, "Catalytic Activity and Effect of Modifiers on Ni-Based Catalysts for the Dry Reforming of Methane", *International Journal of Hydrogen Energy*, Vol. 35, No. 11, pp. 6052-6056, 2010.

44. Kambolis, A., H. Matralis, A. Trovarelli, and C. Papadopoulou, "Ni/CeO_2-ZrO_2 Catalysts for the Dry Reforming of Methane", *Applied Catalysis A: General*, Vol. 377, No. 1–2, pp. 16-26, 2010.

45. Alipour, Z., M. Rezaei, and F. Meshkani, "Effects of Support Modifiers on the Catalytic Performance of Ni/Al_2O_3 Catalyst in CO_2 Reforming of Methane", *Fuel*, Vol. 129, No. 1, pp. 197-203, 2014.

46. Meshkani, F., M. Rezaei, and M. Andache, "Investigation of the Catalytic Performance of Ni/MgO Catalysts in Partial Oxidation, Dry Reforming and Combined Reforming of Methane", *Journal of Industrial and Engineering Chemistry*, Vol. 20, No. 4, pp. 1251-1260, 2014.

47. Alvar, E. N. and M. Rezaei, "Mesoporous Nanocrystalline $MgAl_2O_4$ Spinel and Its Applications as Support for Ni Catalyst in Dry Reforming", *Scripta Materialia*, Vol. 61, No. 2, pp. 212-215, 2009.

48. Hadian, N. and M. Rezaei, "Combination of Dry Reforming and Partial Oxidation of Methane over Ni Catalysts Supported on Nanocrystalline $MgAl_2O_4$", *Fuel*, Vol. 113, No. 1, pp. 571-579, 2013.

49. Chang, J.-S., D.-Y. Hong, X. Li, and S.-E. Park, "Thermogravimetric Analyses and Catalytic Behaviors of Zirconia-Supported Nickel Catalysts for Carbon Dioxide Reforming of Methane", *Catalysis Today*, Vol. 115, No. 1–4, pp. 186-190, 2006.

50. Moniri, A., S. M. Alavi, and M. Rezaei, "Syngas Production by Combined Carbon Dioxide Reforming and Partial Oxidation of Methane over Ni/α-Al_2O_3 Catalysts", *Journal of Natural Gas Chemistry*, Vol. 19, No. 6, pp. 638-641, 2010.

51. Al-Fatesh, A. S. A. and A. H. Fakeeha, "Effects of Calcination and Activation Temperature on Dry Reforming Catalysts", *Journal of Saudi Chemical Society*, Vol. 16, No. 1, pp. 55-61, 2012.

52. García-Diéguez, M., I. S. Pieta, M. C. Herrera, M. A. Larrubia, and L. J. Alemany, "Nanostructured Pt- and Ni-Based Catalysts for CO_2-Reforming of Methane", *Journal of Catalysis*, Vol. 270, No. 1, pp. 136-145, 2010.

53. García-Diéguez, M., I. S. Pieta, M. C. Herrera, M. A. Larrubia, and L. J. Alemany, "Improved Pt-Ni Nanocatalysts for Dry Reforming of Methane", *Applied Catalysis A: General*, Vol. 377, No. 1–2, pp. 191-199, 2010.

54. Yao, L., J. Zhu, X. Peng, D. Tong, and C. Hu, "Comparative Study on the Promotion Effect of Mn and Zr on the Stability of Ni/SiO_2 Catalyst for CO_2 Reforming of Methane", *International Journal of Hydrogen Energy*, Vol. 38, No. 18, pp. 7268-7279, 2013.

55. Zanganeh, R., M. Rezaei, and A. Zamaniyan, "Preparation of Nanocrystalline NiO–MgO Solid Solution Powders as Catalyst for Methane Reforming with Carbon Dioxide: Effect of Preparation Conditions", *Advanced Powder Technology*, Vol. 25, No. 3, pp. 1111-1117, 2014.

56. Zhang, S., J. Wang, H. Liu, and X. Wang, "One-Pot Synthesis of Ni-Nanoparticle-Embedded Mesoporous Titania/Silica Catalyst and Its Application for CO_2-Reforming of Methane", *Catalysis Communications*, Vol. 9, No. 6, pp. 995-1000, 2008.

57. Özkara-Aydınoğlu, Ş. and A. E. Aksoylu, "CO_2 Reforming of Methane over Pt–Ni/Al_2O_3 Catalysts: Effects of Catalyst Composition, and Water and Oxygen Addition to the Feed", *International Journal of Hydrogen Energy*, Vol. 36, No. 4, pp. 2950-2959, 2011.

58. Rezaei, M., S. M. Alavi, S. Sahebdelfar, and Z.-F. Yan, "A Highly Stable Catalyst in Methane Reforming with Carbon Dioxide", *Scripta Materialia*, Vol. 61, No. 2, pp. 173-176, 2009.

59. Al-Fatesh, A., "Suppression of Carbon Formation in CH_4–CO_2 Reforming by Addition of Sr into Bimetallic Ni–Co/γ-Al_2O_3 Catalyst", *Journal of King Saud University - Engineering Sciences*, Vol. 27, No. 1, pp. 101-107, 2013.

60. Wang, N., X. Yu, K. Shen, W. Chu, and W. Qian, "Synthesis, Characterization and Catalytic Performance of MgO-Coated Ni/SBA-15 Catalysts for Methane Dry Reforming to Syngas and Hydrogen", *International Journal of Hydrogen Energy*, Vol. 38, No. 23, pp. 9718-9731, 2013.

61. Liu, D., W. N. E. Cheo, Y. W. Y. Lim, A. Borgna, R. Lau, and Y. Yang, "A Comparative Study on Catalyst Deactivation of Nickel and Cobalt Incorporated MCM-41 Catalysts Modified by Platinum in Methane Reforming with Carbon Dioxide", *Catalysis Today*, Vol. 154, No. 3–4, pp. 229-236, 2010.

62. Tang, M., L. Xu, and M. Fan, "Effect of Ce on 5 wt% Ni/ZSM-5 Catalysts in the CO_2 Reforming of CH_4 Reaction", *International Journal of Hydrogen Energy*, Vol. 39, No. 28, pp. 15482-15496, 2014.

63. Naeem, M. A., A. S. Al-Fatesh, A. E. Abasaeed, and A. H. Fakeeha, "Activities of Ni-Based Nano Catalysts for CO_2–CH_4 Reforming Prepared by Polyol Process", *Fuel Processing Technology*, Vol. 122, No. 1, pp. 141-152, 2014.

64. Ranjbar, A. and M. Rezaei, "Dry Reforming Reaction over Nickel Catalysts Supported on Nanocrystalline Calcium Aluminates with Different CaO/Al_2O_3 Ratios", *Journal of Natural Gas Chemistry*, Vol. 21, No. 2, pp. 178-183, 2012.

65. Wang, Y.-H., H.-M. Liu, and B.-Q. Xu, "Durable Ni/MgO Catalysts for CO_2 Reforming of Methane: Activity and Metal–Support Interaction", *Journal of Molecular Catalysis A: Chemical*, Vol. 299, No. 1–2, pp. 44-52, 2009.

66. Meshkani, F. and M. Rezaei, "Ni Catalysts Supported on Nanocrystalline Magnesium Oxide for Syngas Production by CO_2 Reforming of CH_4", *Journal of Natural Gas Chemistry*, Vol. 20, No. 2, pp. 198-203, 2011.

67. Hadian, N., M. Rezaei, Z. Mosayebi, and F. Meshkani, "CO_2 Reforming of Methane over Nickel Catalysts Supported on Nanocrystalline $MgAl_2O_4$ with High Surface Area", *Journal of Natural Gas Chemistry*, Vol. 21, No. 2, pp. 200-206, 2012.

68. Bellido, J. D. A. and E. M. Assaf, "Effect of the Y_2O_3–ZrO_2 Support Composition on Nickel Catalyst Evaluated in Dry Reforming of Methane", *Applied Catalysis A: General*, Vol. 352, No. 1–2, pp. 179-187, 2009.

69. Pompeo, F., N. N. Nichio, O. A. Ferretti, and D. Resasco, "Study of Ni Catalysts on Different Supports to Obtain Synthesis Gas", *International Journal of Hydrogen Energy*, Vol. 30, No. 13–14, pp. 1399-1405, 2005.

70. Fajardo, H. V., A. O. Martins, R. M. de Almeida, L. K. Noda, L. F. D. Probst, N. L. V. Carreño, and A. Valentini, "Synthesis of Mesoporous Al_2O_3 Macrospheres Using the Biopolymer Chitosan as a Template: A Novel Active Catalyst System for CO_2 Reforming of Methane", *Materials Letters*, Vol. 59, No. 29–30, pp. 3963-3967, 2005.

71. Al-Fatesh, A. S. A., A. H. Fakeeha, and A. E. Abasaeed, "Effects of Selected Promoters on Ni/Y-Al_2O_3 Catalyst Performance in Methane Dry Reforming", *Chinese Journal of Catalysis*, Vol. 32, No. 9–10, pp. 1604-1609, 2011.

72. Juan-Juan, J., M. C. Román-Martínez, and M. J. Illán-Gómez, "Effect of Potassium Content in the Activity of K-Promoted Ni/Al_2O_3 Catalysts for the Dry Reforming of Methane", *Applied Catalysis A: General*, Vol. 301, No. 1, pp. 9-15, 2006.

73. Halliche, D., O. Cherifi, and A. Auroux, "Microcalorimetric Studies and Methane Reforming by CO_2 on Ni-Based Zeolite Catalysts", *Thermochimica Acta*, Vol. 434, No. 1–2, pp. 125-131, 2005.

74. Fakeeha, A. H., W. U. Khan, A. S. Al-Fatesh, and A. E. Abasaeed, "Stabilities of Zeolite-Supported Ni Catalysts for Dry Reforming of Methane", *Chinese Journal of Catalysis*, Vol. 34, No. 4, pp. 764-768, 2013.

75. Vafaeian, Y., M. Haghighi, and S. Aghamohammadi, "Ultrasound Assisted Dispersion of Different Amount of Ni over ZSM-5 Used as Nanostructured Catalyst for Hydrogen Production Via CO_2 Reforming of Methane", *Energy Conversion and Management*, Vol. 76, No. 1, pp. 1093-1103, 2013.

76. Takanabe, K., K. Nagaoka, K. Nariai, and K.-i. Aika, "Titania-Supported Cobalt and Nickel Bimetallic Catalysts for Carbon Dioxide Reforming of Methane", *Journal of Catalysis*, Vol. 232, No. 2, pp. 268-275, 2005.

77. Zanganeh, R., M. Rezaei, A. Zamaniyan, and H. R. Bozorgzadeh, "Preparation of Ni0.1Mg0.9O Nanocrystalline Powder and Its Catalytic Performance in Methane Reforming with Carbon Dioxide", *Journal of Industrial and Engineering Chemistry*, Vol. 19, No. 1, pp. 234-239, 2013.

78. Abdollahifar, M., M. Haghighi, and A. A. Babaluo, "Syngas Production Via Dry Reforming of Methane over Ni/Al_2O_3–MgO Nanocatalyst Synthesized Using Ultrasound Energy", *Journal of Industrial and Engineering Chemistry*, Vol. 20, No. 4, pp. 1845-1851, 2014.

79. González, A. R., Y. J. O. Asencios, E. M. Assaf, and J. M. Assaf, "Dry Reforming of Methane on Ni–Mg–Al Nano-Spheroid Oxide Catalysts Prepared by the Sol–Gel Method from Hydrotalcite-Like Precursors", *Applied Surface Science*, Vol. 280, No. 1, pp. 876-887, 2013.

80. Khajenoori, M., M. Rezaei, and F. Meshkani, "Dry Reforming over CeO_2-Promoted Ni/MgO Nano-Catalyst: Effect of Ni Loading and CH_4/CO_2 Molar Ratio", *Journal of Industrial and Engineering Chemistry*, Vol. 21, No. 1, pp. 717-722, 2015.

81. Xu, J., W. Zhou, Z. Li, J. Wang, and J. Ma, "Biogas Reforming for Hydrogen Production over Nickel and Cobalt Bimetallic Catalysts", *International Journal of Hydrogen Energy*, Vol. 34, No. 16, pp. 6646-6654, 2009.

82. Qian, L., Z. Ma, Y. Ren, H. Shi, B. Yue, S. Feng, J. Shen, and S. Xie, "Investigation of La Promotion Mechanism on Ni/SBA-15 Catalysts in CH_4 Reforming with CO_2", *Fuel*, Vol. 122, No. 1, pp. 47-53, 2014.

83. Luengnaruemitchai, A. and A. Kaengsilalai, "Activity of Different Zeolite-Supported Ni Catalysts for Methane Reforming with Carbon Dioxide", *Chemical Engineering Journal*, Vol. 144, No. 1, pp. 96-102, 2008.

84. Jóźwiak, W. K., M. Nowosielska, and J. Rynkowski, "Reforming of Methane with Carbon Dioxide over Supported Bimetallic Catalysts Containing Ni and Noble Metal: I. Characterization and Activity of SiO_2 Supported Ni–Rh Catalysts", *Applied Catalysis A: General*, Vol. 280, No. 2, pp. 233-244, 2005.

85. Taufiq-Yap, Y. H., Sudarno, U. Rashid, and Z. Zainal, "CeO_2–SiO_2 Supported Nickel Catalysts for Dry Reforming of Methane toward Syngas Production", *Applied Catalysis A: General*, Vol. 468, No. 1, pp. 359-369, 2013.

86. Wu, H., G. Pantaleo, V. La Parola, A. M. Venezia, X. Collard, C. Aprile, and L. F. Liotta, "Bi- and Trimetallic Ni Catalysts over Al_2O_3 and Al_2O_3-Mox (M=Ce or Mg) Oxides for Methane Dry Reforming: Au and Pt Additive Effects", *Applied Catalysis B: Environmental*, Vol. 156–157, No. 1, pp. 350-361, 2014.

87. Ocsachoque, M., F. Pompeo, and G. Gonzalez, "Rh–Ni/CeO_2–Al_2O_3 Catalysts for Methane Dry Reforming", *Catalysis Today*, Vol. 172, No. 1, pp. 226-231, 2011.

88. Bellido, J. D. A., J. E. De Souza, J.-C. M'Peko, and E. M. Assaf, "Effect of Adding CaO to ZrO_2 Support on Nickel Catalyst Activity in Dry Reforming of Methane", *Applied Catalysis A: General*, Vol. 358, No. 2, pp. 215-223, 2009.

89. Nagaraja, B. M., D. A. Bulushev, S. Beloshapkin, and J. R. H. Ross, "The Effect of Potassium on the Activity and Stability of Ni–MgO–ZrO_2 Catalysts for the Dry Reforming of Methane to Give Synthesis Gas", *Catalysis Today*, Vol. 178, No. 1, pp. 132-136, 2011.

90. Rezaei, M., S. M. Alavi, S. Sahebdelfar, and Z.-F. Yan, "Effects of CO_2 Content on the Activity and Stability of Nickel Catalyst Supported on Mesoporous Nanocrystalline Zirconia", *Journal of Natural Gas Chemistry*, Vol. 17, No. 3, pp. 278-282, 2008.

91. Al–Fatish, A. S. A., A. A. Ibrahim, A. H. Fakeeha, M. A. Soliman, M. R. H. Siddiqui, and A. E. Abasaeed, "Coke Formation During CO_2 Reforming of CH_4 over Alumina-Supported Nickel Catalysts", *Applied Catalysis A: General*, Vol. 364, No. 1–2, pp. 150-155, 2009.

92. Hou, Z., P. Chen, H. Fang, X. Zheng, and T. Yashima, "Production of Synthesis Gas Via Methane Reforming with CO_2 on Noble Metals and Small Amount of Noble-(Rh-) Promoted Ni Catalysts", *International Journal of Hydrogen Energy*, Vol. 31, No. 5, pp. 555-561, 2006.

93. Habibi, N., M. Rezaei, N. Majidian, and M. Andache, "CH_4 Reforming with CO_2 for Syngas Production over La_2O_3 Promoted Ni Catalysts Supported on Mesoporous Nanostructured ᵞ-Al_2O_3", *Journal of Energy Chemistry*, Vol. 23, No. 4, pp. 435-442, 2014.

94. Newnham, J., K. Mantri, M. H. Amin, J. Tardio, and S. K. Bhargava, "Highly Stable and Active Ni-Mesoporous Alumina Catalysts for Dry Reforming of Methane", *International Journal of Hydrogen Energy*, Vol. 37, No. 2, pp. 1454-1464, 2012.

95. Damyanova, S., B. Pawelec, K. Arishtirova, and J. L. G. Fierro, "Biogas Reforming over Bimetallic PdNi Catalysts Supported on Phosphorus-Modified Alumina", *International Journal of Hydrogen Energy*, Vol. 36, No. 17, pp. 10635-10647, 2011.

96. García-Diéguez, M., E. Finocchio, M. Á. Larrubia, L. J. Alemany, and G. Busca, "Characterization of Alumina-Supported Pt, Ni and PtNi Alloy Catalysts for the Dry Reforming of Methane", *Journal of Catalysis*, Vol. 274, No. 1, pp. 11-20, 2010.

97. Mirzaei, F., M. Rezaei, F. Meshkani, and Z. Fattah, "Carbon Dioxide Reforming of Methane for Syngas Production over Co–MgO Mixed Oxide Nanocatalysts", *Journal of Industrial and Engineering Chemistry*, Vol. 21, No. 1, pp. 662-667, 2014.

98. Nematollahi, B., M. Rezaei, M. Asghari, A. Fazeli, E. N. Lay, and F. Nematollahi, "A Comparative Study between Modeling and Experimental Results over Rhodium Supported Catalyst in Dry Reforming Reaction", *Fuel*, Vol. 134, No. 1, pp. 565-572, 2014.

99. Fakeeha, A. H., M. A. Naeem, W. U. Khan, and A. S. Al-Fatesh, "Syngas Production Via CO_2 Reforming of Methane Using Co-Sr-Al Catalyst", *Journal of Industrial and Engineering Chemistry*, Vol. 20, No. 2, pp. 549-557, 2014.

100. Lee, J.-H., Y.-W. You, H.-C. Ahn, J.-S. Hong, S.-B. Kim, T.-S. Chang, and J.-K. Suh, "The Deactivation Study of Co–Ru–Zr Catalyst Depending on Supports in the Dry Reforming of Carbon Dioxide", *Journal of Industrial and Engineering Chemistry*, Vol. 20, No. 1, pp. 284-289, 2014.

101. Shi, C. and P. Zhang, "Effect of a Second Metal (Y, K, Ca, Mn or Cu) Addition on the Carbon Dioxide Reforming of Methane over Nanostructured Palladium Catalysts", *Applied Catalysis B: Environmental*, Vol. 115–116, No. 1, pp. 190-200, 2012.

102. Ballarini, A., F. Basile, P. Benito, I. Bersani, G. Fornasari, S. de Miguel, S. C. P. Maina, J. Vilella, A. Vaccari, and O. A. Scelza, "Platinum Supported on Alkaline and Alkaline Earth Metal-Doped Alumina as Catalysts for Dry Reforming and Partial Oxidation of Methane", *Applied Catalysis A: General*, Vol. 433–434, No. 1, pp. 1-11, 2012.

103. Sarusi, I., K. Fodor, K. Baán, A. Oszkó, G. Pótári, and A. Erdőhelyi, "CO_2 Reforming of CH_4 on Doped Rh/Al_2O_3 Catalysts", *Catalysis Today*, Vol. 171, No. 1, pp. 132-139, 2011.

104. Shang, R., X. Guo, S. Mu, Y. Wang, G. Jin, H. Kosslick, A. Schulz, and X.-Y. Guo, "Carbon Dioxide Reforming of Methane to Synthesis Gas over Ni/Si_3N_4 Catalysts", *International Journal of Hydrogen Energy*, Vol. 36, No. 8, pp. 4900-4907, 2011.

105. Nematollahi, B., M. Rezaei, and M. Khajenoori, "Combined Dry Reforming and Partial Oxidation of Methane to Synthesis Gas on Noble Metal Catalysts", *International Journal of Hydrogen Energy*, Vol. 36, No. 4, pp. 2969-2978, 2011.

106. San José-Alonso, D., M. J. Illán-Gómez, and M. C. Román-Martínez, "K and Sr Promoted Co Alumina Supported Catalysts for the CO_2 Reforming of Methane", *Catalysis Today*, Vol. 176, No. 1, pp. 187-190, 2011.

107. Reddy, G. K., S. Loridant, A. Takahashi, P. Delichère, and B. M. Reddy, "Reforming of Methane with Carbon Dioxide over Pt/ZrO_2/SiO_2 Catalysts—Effect of Zirconia to Silica Ratio", *Applied Catalysis A: General*, Vol. 389, No. 1–2, pp. 92-100, 2010.

108. Damyanova, S., B. Pawelec, K. Arishtirova, M. V. M. Huerta, and J. L. G. Fierro, "The Effect of CeO_2 on the Surface and Catalytic Properties of Pt/CeO_2–ZrO_2 Catalysts for Methane Dry Reforming", *Applied Catalysis B: Environmental*, Vol. 89, No. 1–2, pp. 149-159, 2009.

109. Li, X., Q. Hu, Y. Yang, J. Chen, and Z. Lai, "Effects of Sol-Gel Method and Lanthanum Addition on Catalytic Performances of Nickel-Based Catalysts for Methane Reforming with Carbon Dioxide", *Journal of Rare Earths*, Vol. 26, No. 6, pp. 864-868, 2008.

110. Wang, R., X. Liu, Y. Chen, W. Li, and H. Xu, "Effect of Metal–Support Interaction on Coking Resistance of Rh-Based Catalysts in CH_4/CO_2 Reforming", *Chinese Journal of Catalysis*, Vol. 28, No. 10, pp. 865-869, 2007.

111. Rezaei, M., S. M. Alavi, S. Sahebdelfar, and Z.-F. Yan, "Syngas Production by Methane Reforming with Carbon Dioxide on Noble Metal Catalysts", *Journal of Natural Gas Chemistry*, Vol. 15, No. 4, pp. 327-334, 2006.

112. Yang, M. and H. Papp, "CO_2 Reforming of Methane to Syngas over Highly Active and Stable Pt/MgO Catalysts", *Catalysis Today*, Vol. 115, No. 1–4, pp. 199-204, 2006.

113. Ballarini, A. D., S. R. de Miguel, E. L. Jablonski, O. A. Scelza, and A. A. Castro, "Reforming of CH_4 with CO_2 on Pt-Supported Catalysts: Effect of the Support on the Catalytic Behaviour", *Catalysis Today*, Vol. 107–108, No. 1, pp. 481-486, 2005.

114. Bouarab, R., O. Cherifi, and A. Auroux, "Effect of the Basicity Created by La_2O_3 Addition on the Catalytic Properties of Co(O)/SiO_2 in CH_4+CO_2 Reaction", *Thermochimica Acta*, Vol. 434, No. 1–2, pp. 69-73, 2005.